THE FOCUSING OF CYLINDRICAL ELECTRON BEAMS WITH PERIODIC MAGNETIC FIELDS

by
E. H. Blevis

A Thesis submitted to the Faculty of Graduate Studies and Research at McGill University in partial fulfillment of the requirements of the degree of Master of Science.

The Eaton Electronics Research Laboratory,
Department of Physics
McGill University

April 1956

TABLE OF CONTENTS

I.	Introduction	1
II.	Theory	3
	2.1 Equation for the Trajectory of an Edge Electron	3
	2.2 Analysis of Beam Profile Curves	5
	2.3 Stability of Flow	10
	2.4 Positive Ions	11
III.	Experimental Apparatus	12
	3.1 The Electron Gun	12
	3.2 The Hard Vacuum Tube	12
	3.3 The Periodic Magnet Structures	16
	3.4 The Associated Circuits	20
IV.	Experimental Results	24
	4.1 Steady-State Measurements	24
	4.2 Pulsed Measurements	32
V.	Summary and Conclusions	35
VI.	Acknowledgements	36
VII.	Bibliography	37

I. INTRODUCTION

The problem of generating long cylindrical electron beams of almost constant diameter has received much attention in recent years. Space charge spreading due to the repulsion of the like charges in the beam must be eliminated by an external focusing field. Sets of widely spaced electrostatic or magnetostatic lenses (15) have been used where charge densities were low, while uniform longitudinal magnetic fields (2, 15) have been used where charge densities were high. J.R. Pierce (5), in a Letter to the Editor of the Journal of Applied Physics, September 1953, suggested that spatially alternating magnetic fields could be used to advantage in place of the uniform magnetic fields. Considerable saving in weight of magnetic material can be thus achieved; because the mean square field, which appears in the equations describing the focusing action of the magnetic field, is higher per unit weight for the alternating field than for the uniform field.

Recent efforts to extend the frequency of operation and to increase the available power of existing microwave devices of the traveling wave and backward wave types, has placed additional emphasis on the focusing problem. These devices depend on the interaction of a well behaved electron beam with a rigid circuit structure. The structure may be one of the many detailed forms described in the literature (14), for example a helix; but will in many cases, consist in basic form of a long conducting cylinder of constant diameter. To achieve low noise operation consistent with efficient interaction, it is necessary to pass the electron beam as close to the walls of this conducting cylinder as possible, while keeping the number of electrons striking the walls low. The diameter of this conducting cylinder, and hence the diameter of the electron beam, will be determined essentially by the operating frequency and voltage of the device. Higher frequencies and lower voltages require smaller diameters. If one wishes to increase the frequency of an existing device by geometric scaling while holding the voltage constant, one must increase the charge density in order to maintain the same power. To increase the power while maintaining the voltage and the frequency constant, one must again increase the charge density. Both of these operations make the focusing problem more acute. During the last year, several packaged units incorporating spatially alternating magnetic fields have appeared in the literature (13, 14).

J.T. Mendel et al (7), May 1954, reported a simple theory and experiment using an axially symmetric periodic magnetic field. A more complete theory dealing with both axially symmetric and quadrupolar periodic magnetic fields was published by A.M. Clogston et al (8) in April 1954. The optimum design of a periodic permanent magnet structure was discussed by K.K.N. Chang (11), March 1955.

The purpose of the author's work described in this thesis was to review and extend the existing theoretical and experimental work on axially symmetric periodic magnetic field focusing. With this intention, an electron gun was designed. This gun produced an external beam of known shape, while giving current densities typical of those found in modern traveling wave tubes. A hard type vacuum tube incorporating the gun, a long conducting cylinder, and an electron collector was constructed. A permanent magnet and an electromagnet structure were built. Observations taken under both static and pulsed operating conditions are recorded and discussed in terms of the theory. Finally, where the theory proves inadequate, suggestions are made towards an improved theory and an experiment to test this improved theory.

II. THEORY

Assuming laminar flow and a magnetically shielded cathode, an equation describing the trajectory of an edge electron in the beam is found. Beam profile curves obtained by solving this equation on an analog computer in the laboratory are analysed. Conclusions are drawn regarding the stability of the flow and the effect of entry conditions into the magnetic field.

2.1 Equation for the Trajectory of an Edge Electron

The analysis presented here will follow closely that first presented by Clogston and Heffner (8).

From the Lorentz force equation, the force, $\vec{F}$, on an electron is given by

$$\vec{F} = -e\left[\vec{E} + (\vec{v} \times \vec{B})\right] \qquad 1$$

Using cylindrical coordinates the components of $\vec{F}$ are

$$\left.\begin{aligned} F_r &= m(\ddot{r} - r\dot{\theta}^2) \\ F_\theta &= \frac{1}{r}\frac{d}{dt}(mr^2\dot{\theta}) \\ F_z &= m\ddot{z} \end{aligned}\right\} \qquad 2$$

Now consider systems of cylindrical symmetry with $\vec{B}$ given by

$$\vec{B} = B_o \cos kz \qquad 3$$

where $k = \frac{2\pi}{p}$ and p is the period of the magnetic field. Combining 1 and 2 gives the set of equations

$$\ddot{z} = \eta E_z \qquad 4$$

$$\frac{1}{r}\frac{d}{dt}(r^2\dot{\theta}) = \eta B\dot{r} \qquad 5$$

$$\ddot{r} = \eta E_r - \eta r\dot{\theta}B + r\dot{\theta}^2 \qquad 6$$

where $\eta = e/m$.

Integrating 5 with the boundary condition that at the cathode $\dot{\theta} = 0$, $B = 0$ one obtains

$$\dot{\theta} = \eta \frac{B}{2}$$

Substituting 7 in 6 leads to

$$\ddot{r} + \left(\frac{\eta B}{2}\right)^2 + \eta E_r = 0 \qquad 8$$

Assume that: (1) The electrons on the outside surface of the beam always remain the outermost electrons, i.e. laminar flow. (2) Axial variations of the beam are small and occur in a distance large compared to the diameter of the beam. (3) Axial velocities of the electrons are constant throughout the beam.

Using the second assumption and applying Gauss' law, gives the radial electric field, E_r, on the outside surface of the beam.

$$2\pi r \varepsilon_o E_r = \int \rho \, ds \qquad 9$$

where ε_o is the dielectric constant of free space, ρ is the charge density and ds is the element of area. Because of assumptions (1) and (3), $\int \rho \, ds$ must be a constant. Define the radius of the beam at z = 0 by r_o and the average charge density at the point by

$$\int \rho \, ds = \pi r_o^2 \rho_{av} \qquad 10$$

Also define the plasma frequency

$$\omega_\rho^2 = \frac{\eta \rho_{av}}{\varepsilon_o} \qquad 11$$

Combining 9, 10 and 11 and substituting in 8 one has

$$\ddot{r} + r\left(\frac{\eta B}{2}\right)^2 - r_o^2 \frac{\omega_\rho^2}{2r} = 0 \qquad 12$$

Define a radian frequency ω_c by the equation

$$\omega_c^2 = \frac{1}{2} (\eta B_o)^2 \qquad 13$$

Substitute 13 in 12 to obtain

$$\ddot{r} + r\,\omega_c^2 \cos^2 kz - \frac{r_o^2 \omega_\rho^2}{2r} = 0 \qquad 14$$

If v is the constant velocity of assumption (3) one has t = z/v. Define the radian frequency at which the field appears to alternate as one moves with the electrons as ω_L. In addition place kz = x and kr = y.

Equation 14 then becomes

$$\frac{d^2y}{dx^2} + \left[\frac{1}{2}\frac{\omega_c^2}{\omega_L^2}\cos^2 x\right] y - \frac{1}{2}\left(\frac{\omega_\rho}{\omega_L}\right)^2 \frac{y_o^2}{y} = 0 \qquad 15$$

Place

$$A = \frac{1}{4}\frac{\omega_c^2}{\omega_L^2}, \quad B = \frac{1}{2}\frac{\omega_\rho^2}{\omega_L^2} \qquad \sigma = \frac{y}{y_o} \qquad 16$$

and expand the cosine term to obtain

$$\frac{d^2\sigma}{dx^2} + A(1 + \cos 2x)\sigma - \frac{B}{\sigma} = 0 \qquad 17$$

Note that the magnetic field was chosen to be a maximum at $x = 0$.

2.2.1 Analysis of Beam Profile Curves for $\sigma_o = 1$ and $\left(\frac{d\sigma}{dx}\right)_{x=0} = 0$

Consider first the case where the electrons are introduced at $x = 0$ with parallel motion so that $\sigma_o = 1$ and $\left(\frac{d\sigma}{dx}\right)_{x=0} = 0$. Typical beam profile curves for this case are shown in fig. 1 for six values of the parameters A and B. These curves were taken by the author with the help of G. Farnell on an analog computer designed and built by G. Farnell and now operating in the laboratory. The analog computer scale factors to be used with these curves are

$$\Sigma = \frac{2}{3}\sigma \qquad X = \frac{.199}{3}x \qquad 18$$

where the curved chart lines represent X = constant and the straight chart lines represent Σ = constant. The parameter Q in fig. 1 arises from solving the more general equation

$$\frac{d^2\sigma}{dx^2} + (A + Q\cos 2x)\sigma - \frac{B}{\sigma} = 0 \qquad 19$$

The periodic axially symmetric system of principal interest in this thesis is described by setting $Q = A$ in equation 19, which then reduces to equation 17. The uniform magnetic field (Brillouin field) system treated by Szabo (12), is described by $Q = 0$, while the complementary field system treated by Chang (9) is described by $Q < A$ and $Q \neq A$. This is summarized in table 1.

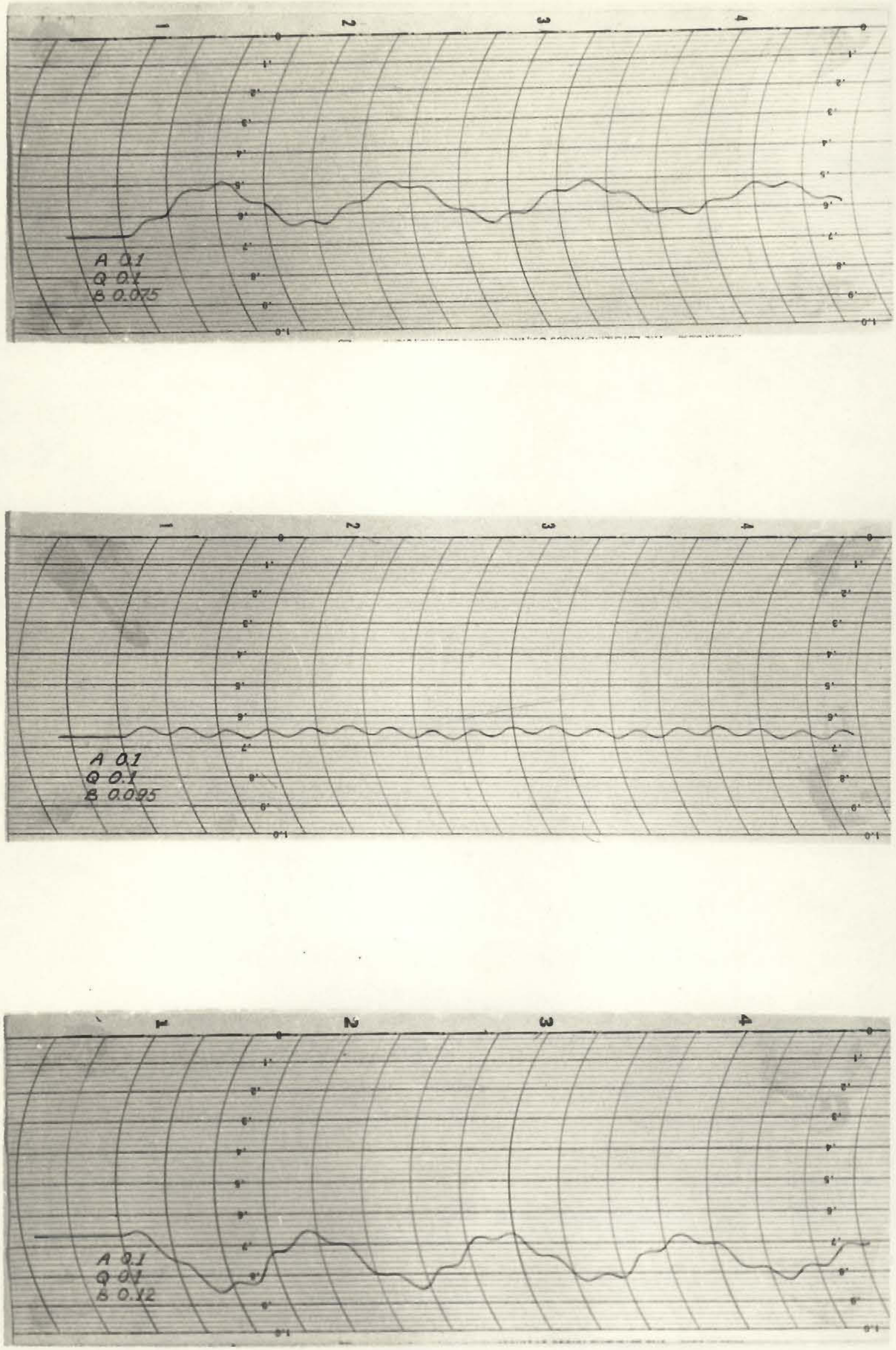

FIG. 1

BEAM PROFILE CURVES

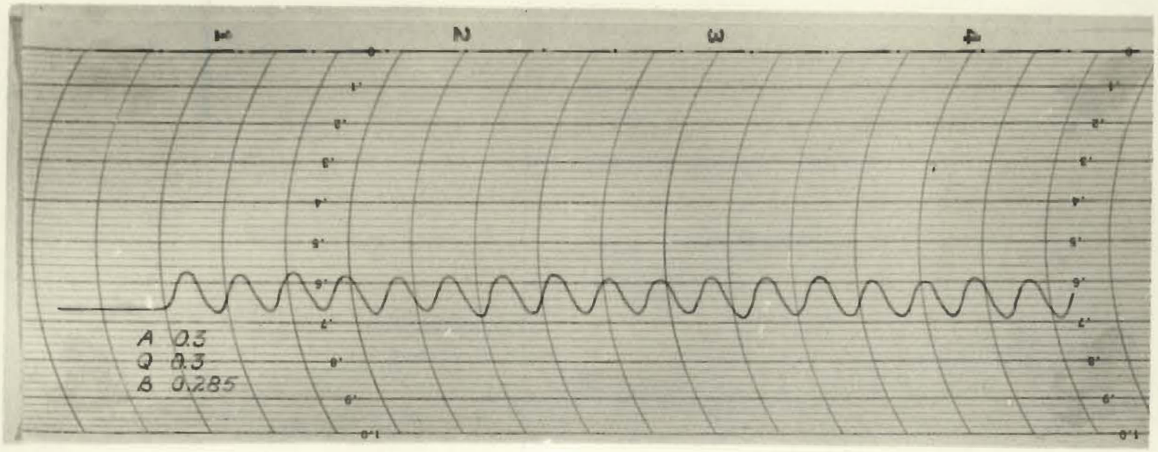

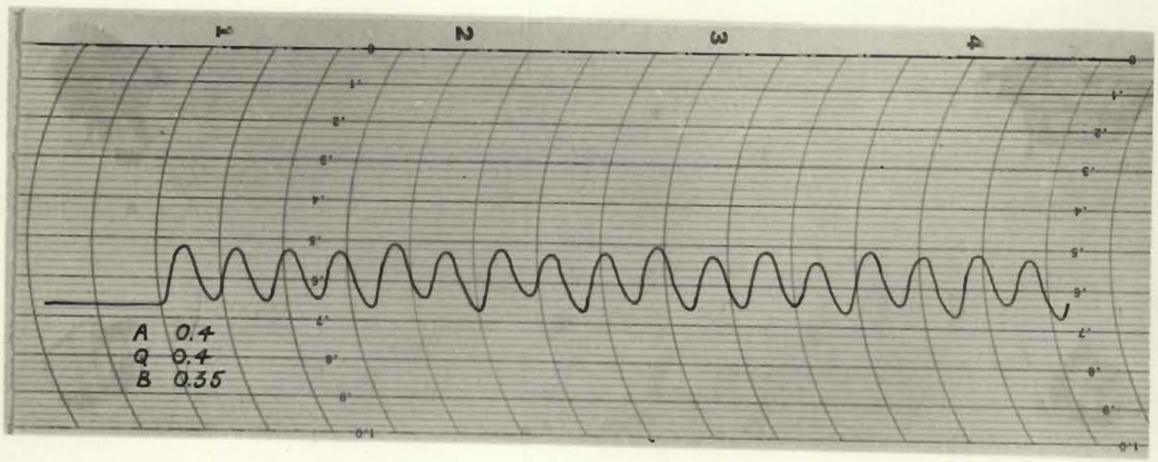

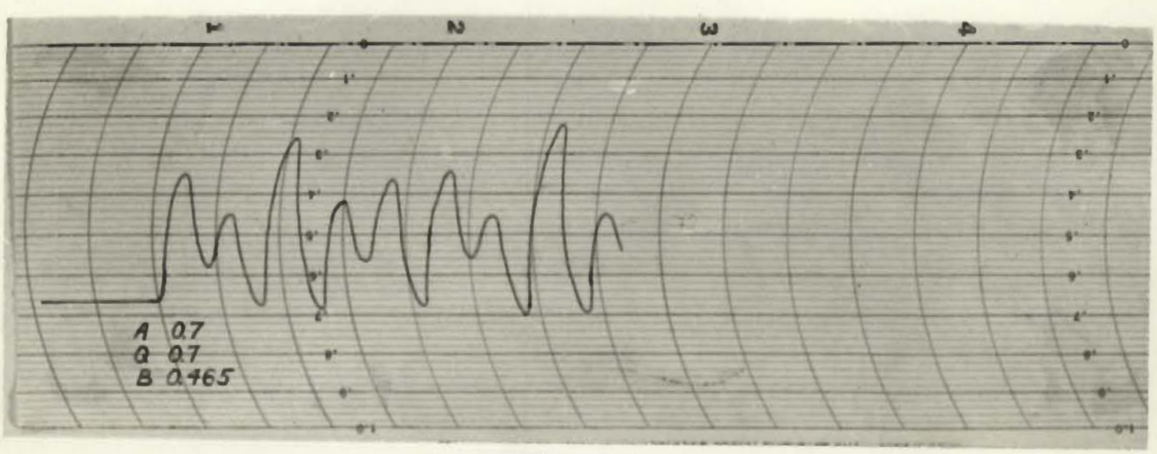

FIG. 1 (CONT.)

BEAM PROFILE CURVES

Solutions of equation 19 for small values of the parameters, that is A, Q, and B less than .6 are characterized approximately by a linear superposition of two 'scallops'. The first scallop has a period which is independent of the values of the parameters and has an amplitude dependent on Q but not dependent on A,B. The period of this scallop is related to the period of the focusing system through the relation $x = ky$. Only when $Q = 0$, that is the uniform field case, does this scallop disappear. In fig. 2 the amplitude of the first scallop is plotted against Q for values of Q from zero to .5.

Field	Relation between Q and A
Uniform	$Q = 0$
Complementary	$Q < A, \quad Q \neq A$
Periodic	$Q = A$

Table 1

The Value of Q in Equation 19 for Different Field Configurations

The second scallop has a period which is dependent on A and an amplitude which is dependent on A and B but is not dependent on Q. The angular frequency of this scallop is related to the Brillouin angular frequency ω_B (12). When the scallop is small, the angular frequency is just $\sqrt{2}$ times the rms cyclotron frequency $\omega_c = \eta\ B_{rms}$ corresponding exactly to the Brillouin frequency. When A and B are adjusted according to the relation plotted in fig. 3, the amplitude of this scallop becomes zero. This situation is called optimum focusing since it produces the most nearly parallel beam. A second important property of this scallop is that it never causes the beam to cross the line $\sigma = 1$, that is the beam input radius. It will be shown later that under certain entry conditions a third scallop is produced which causes the beam to cross its input radius. No adjustment of A and/or B will remove a scallop which causes the beam to cross its input radius.

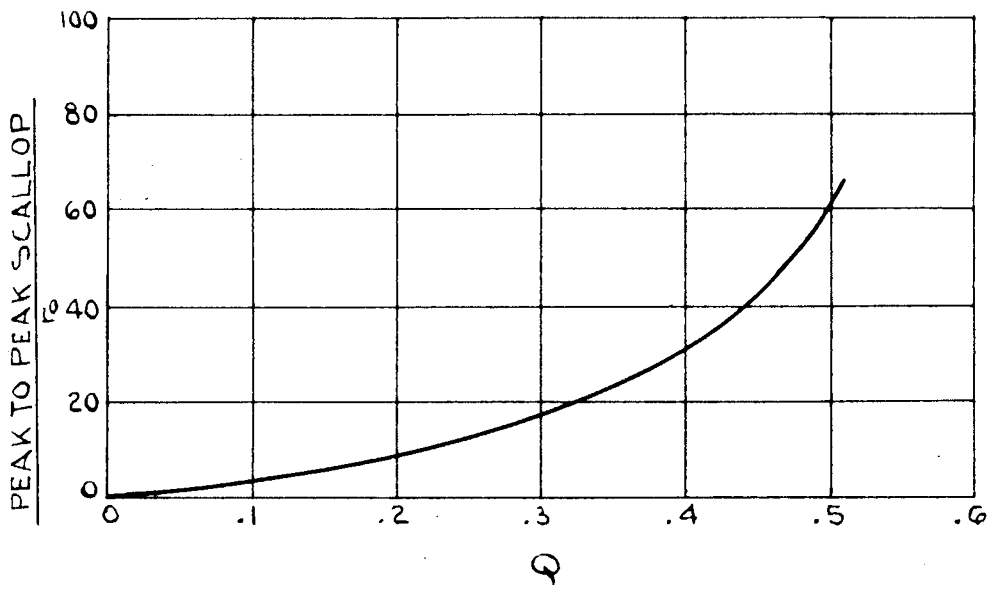

FIG. 2
AMOUNT OF TYPE I SCALLOP

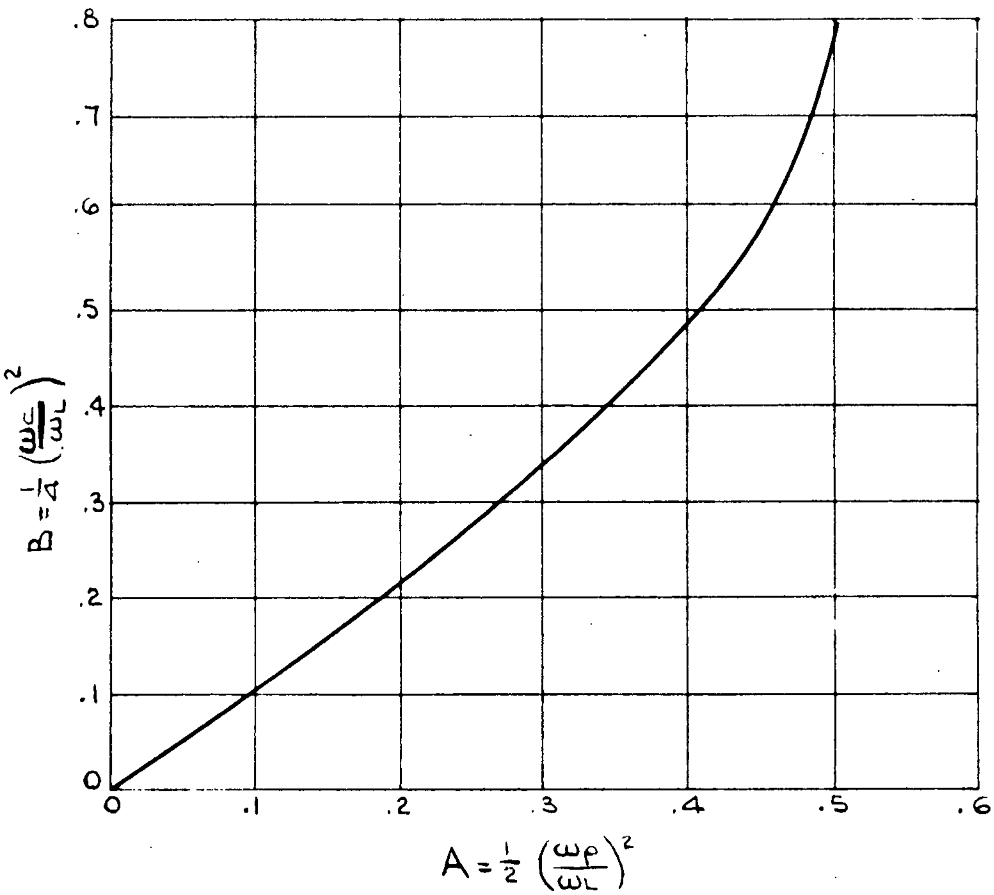

FIG. 3
CONDITION FOR NO TYPE 2 SCALLOP

The effect of a change in σ_0, i.e. a change in the beam radius at $z = 0$ is shown analytically by the following

$$\frac{d^2\sigma'}{dx^2} + (A + Q \cos 2x)\sigma' - \frac{B}{\sigma'} = 0 \qquad 20$$

Let $\sigma' = \lambda\sigma$, λ = constant

$$\lambda\left\{\frac{d^2\sigma}{dx^2} + (A + Q \cos 2x)\sigma\right\} + \frac{B}{\lambda\sigma} = 0 \qquad 21$$

Set $B' = \lambda^2 B$, equation 21 then reduces to equation 19. This can be summarized by saying optimum focusing or any other focusing condition will be reproduced except for a scale factor, λ, if A and Q are held constant and B is changed to $\lambda^2 B$ or if B is held constant and A and Q are changed to A/λ^2 and Q/λ^2 respectively.

2.2.2 Effects of $(\frac{d\sigma}{dx}) \neq 0$ and/or Magnetic Field Not Maximum at $x = 0$

If $(\frac{d\sigma}{dx})_{x=0} \neq 0$, a third scallop will be produced which causes the beam to cross its input radius. Introducing an arbitrary phase angle into the cosine term of equation 19, i.e. having a magnetic field which is not maximum at $x = 0$ will also produce a scallop of the third type. These two effects can be balanced to produce optimum focusing under some conditions. The foregoing statement points out the fact that the electrons may be introduced anywhere along the trajectories obtained in section 2.2.1 provided they are given the slope corresponding to that point. Experimentally it will be found convenient to introduce the electrons at a point where the field is zero. In this case for a value of $A = .1$, the beam must be 3^o divergent.

2.3 Stability of Flow

Contrary to what previous authors have reported, equation 19 has no instability at $A = .66$ as does the corresponding Mathieu equation 22.

$$\frac{d^2\sigma}{dx^2} + (A + Q \cos 2x)\sigma = 0 \qquad A = Q \qquad 22$$

The instability in the Mathieu equation is an exponentially growing sinusoidal.

The growth is prevented in equation 19 by the $\frac{-B}{\sigma}$ term which becomes infinitely large for finite B as σ tries to go to zero. What happens, in fact, is that the solution to equation 19 becomes a growing then decaying sinusoidal. Experimentally, however, stable flow cannot be expected beyond A $\doteq$ .5 because the large scallop of the first type present beyond this point causes the assumption of laminar flow to be invalid. One might expect, however, that stable flow will exist for much higher values of A corresponding to the pass bands of the Mathieu equation.

2.4 Positive Ions

In section 2.1 it was assumed that no positive ions are present in the beam. Experimentally this condition cannot be observed. This problem cannot be solved analytically since it corresponds to a three body problem. When it is assumed that positive ions do not interact with other positive ions, three froces are still present: (1) the force of the applied fields on the electron, (2) the force between electrons, and (3) the force between electron and positive ion. Approximate solutions can be obtained by assuming a fixed simple positive ion distribution. Previous authors have treated the case where the positive ions are assumed to form a fixed uniform plasma. More exact solutions could be obtained by a self consistent field technique. This would involve setting up a positive ion distribution which was complimentary to the potential distribution obtained for the case where positive ions are absent. One would then solve the problem again assuming this distribution and obtain a new potential distribution. This process would be repeated until a self consistent potential was found. The problem is not solved here but is posed in the hope that it will receive more attention in the near future. Because of the presence of positive ions, it will take a finite time for an equilibrium condition to be reached in a practical tube. Indications by previous workers are that times of the order of 10 μsecs might be expected.

III. EXPERIMENTAL APPARATUS

A convergent gun which approximated the Pierce type was built and tested. This gun was incorporated in a hard vacuum tube. Two periodic magnet structures were assembled. Associated circuits were set up which would permit steady state and pulsed measurements to be made.

3.1 The Electron Gun

It was desirable to have a gun which would approximate the Pierce type at some mid-operating point and which would produce a wide range of perveance. The gun had to produce an external beam which had an accessible minimum remote from the anode and was at least three degrees convergent at the anode. A theoretical design for a three electrode gun (design by C. Tunis of this Laboratory), in which the conventional Pierce cathode was replaced by a negative control grid, met the design requirements. Fig. 4 shows in outline this design which was rechecked by the author in an electrolytic tank. Work by C. Tunis indicated that this gun should produce an external beam with a minimum diameter of 2 mm. located 10 mm. from the anode aperture. The anode was stamped out of .017 inch monel metal sheet (type 326 non-magnetic). The control grid, shown in detail in fig. 5, was also worked from non-magnetic monel metal. Oxide coated 3 mm. cathode buttons were prepared. The gun was then assembled using three alundum rods to align and space the electrodes. These rods also served to fix the gun relative to the completed tube as indicated below.

3.2 The Hard Vacuum Tube

The tube was assembled around a long cylindrical molybdenum tube which served as an electric field free drift space. A monel metal flange carrying three holes to receive the alundum rods of the gun was welded to the end of the molybdenum tube. The complete assembly consisting of electron gun and

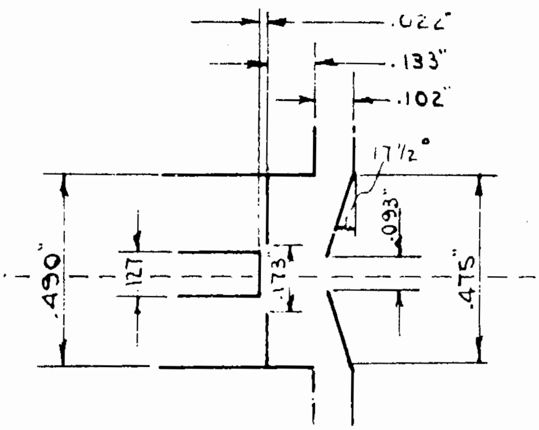

FIG. 4
OUTLINE OF THE GUN

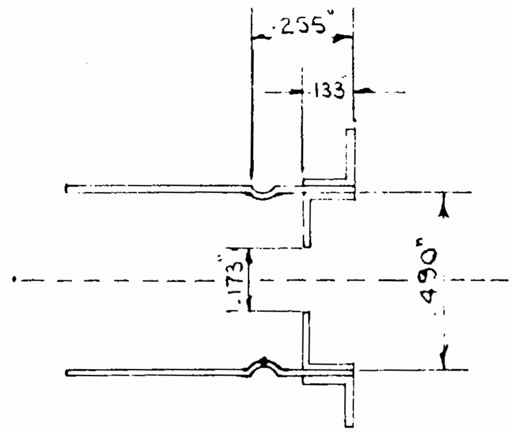

.017" MONEL SHEET
FIG. 5
DETAIL OF THE GRID

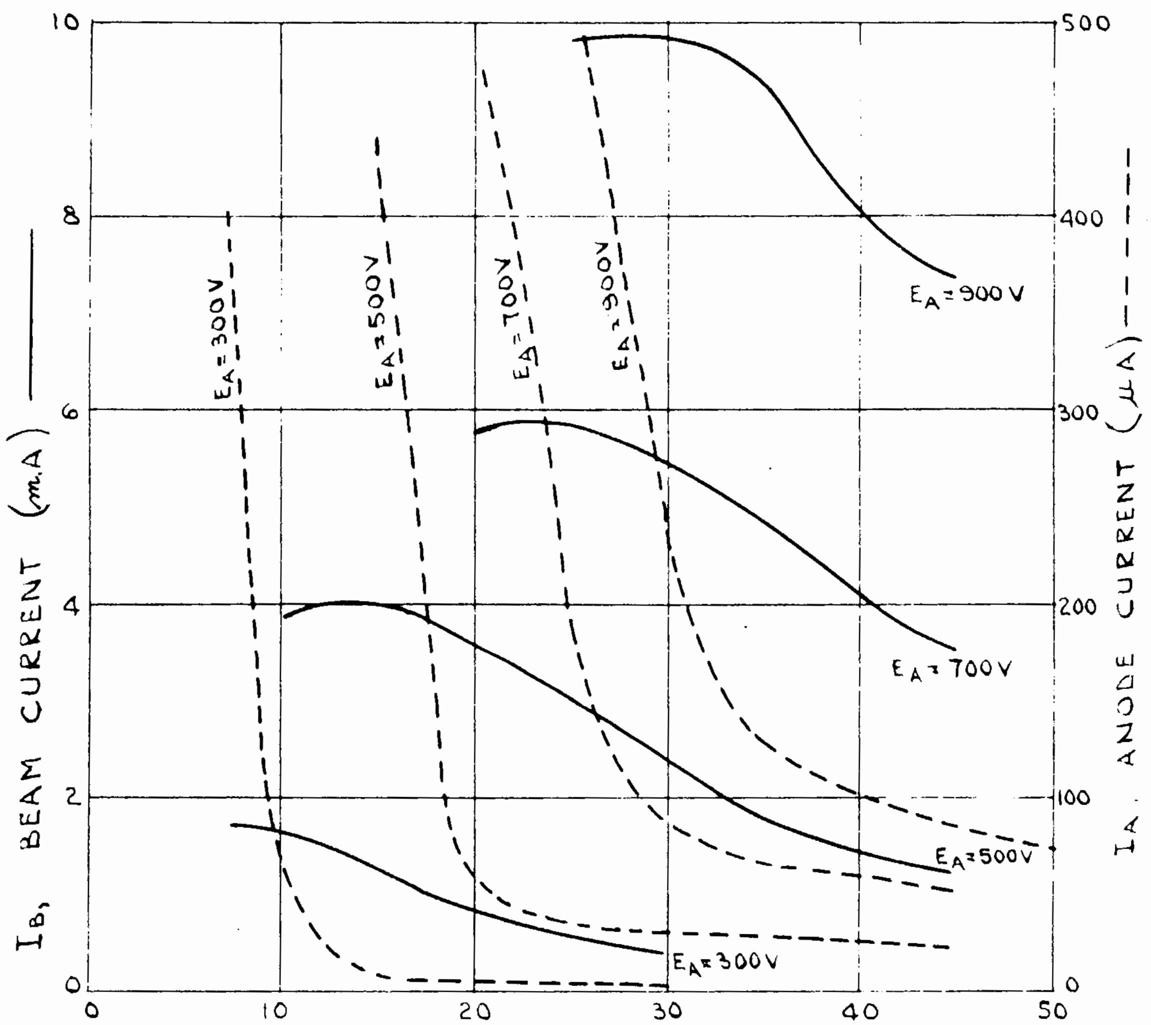

FIG. 6
STATIC CHARACTERISTICS OF THE GUN

drift tube was housed in a pyrex glass envelope which also carried a getter tube, exhaust tube, and kovar electron collector. All metal parts except the cathode button were cleaned in carbon tetrachloride, acetone and alcohol and then heat treated at 900 C. in a hydrogen atmosphere before assembly. The cathode button was prepared for coating by cleaning in a 5% solution of acetic acid. R.C.A. type C-52 cathode coating was used. The heater was of a commercial type designed for use with the standard 3 mm. cathode and was rated at 6.3 V. 600 mA. The molybdenum cylinder with the gun in place is shown in the lower part of fig. 7. Immediately above it the glass envelope with the kovar collector is shown. These two parts are sealed together to form an assembled tube as shown in fig. 8.

The tube was exhausted on a vacuum system consisting of a fore-pump and a three stage water cooled fractionating pump. Octoil-S was used as the pump fluid. The processing, activating and the aging schedule employed is listed below:

(i) Pump on.

(ii) Bake out at 250 C.for 12 hours.

(iii) Bake out at 450 C. for 2 hours.

(iv) Place liquid nitrogen trap on system.

(v) Bake out at 450 C. for 15 minutes.

(vi) Cool to room temperature slowly.

(vii) Apply heater voltage at the rate of 2V./min. until 14V. is reached.

(viii) Two minutes after reaching 14V. apply 40 V.A.C. between cathode and all other elements including grid.

(ix) Check for cathode emission.

(x) Remove all voltages.

(xi) After 15 minutes, heat getters to red temperature without flashing.

(xii) After 5 minutes, flash getters.

(xiii) Seal off immediately.

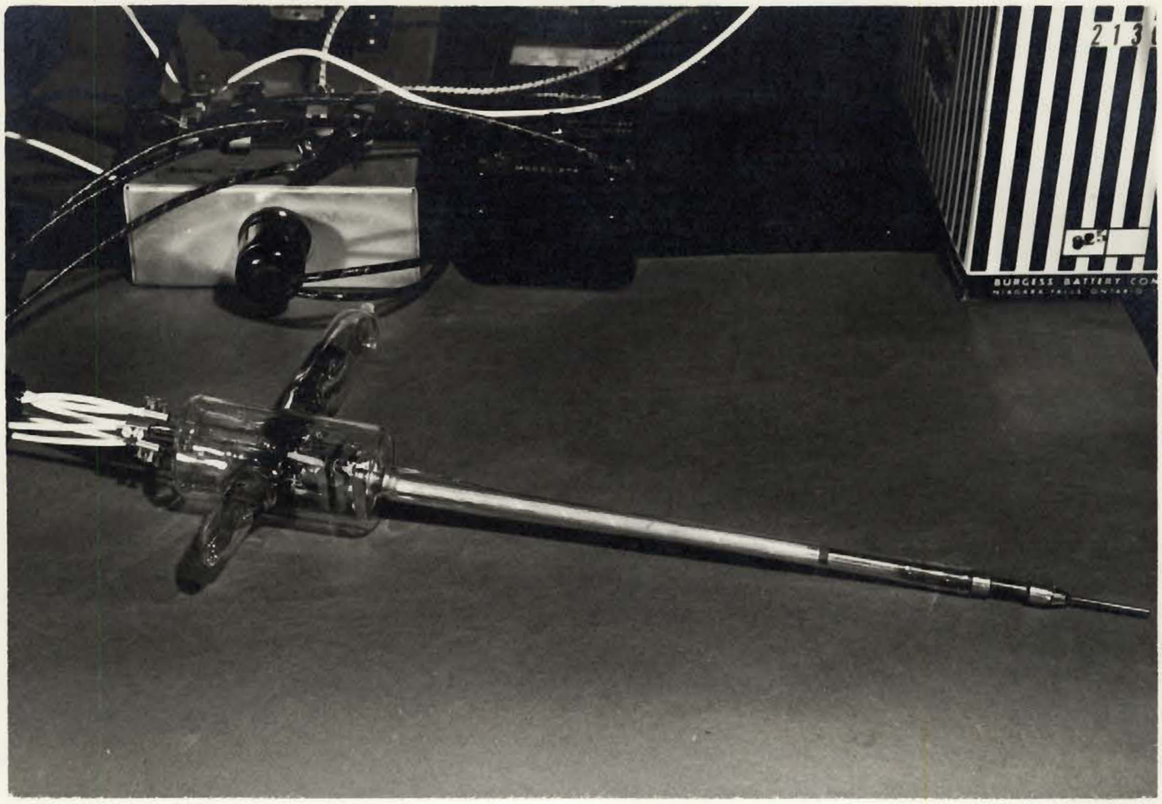

FIG. 8

COMPLETED AND PROCESSED TUBE

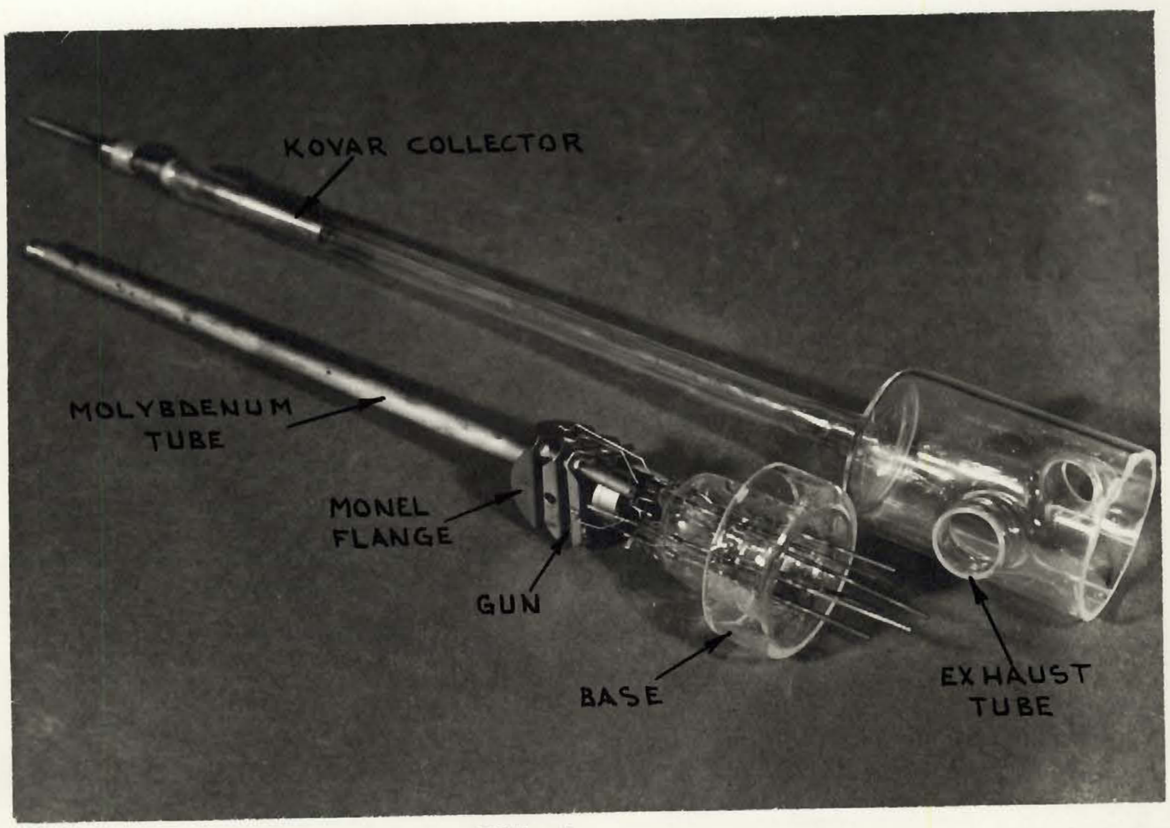

FIG. 7

TUBE PRIOR TO SEALING

(xiv) Pump off.

(xv) Age with 14V. on heater and 40 V.A.C. between cathode and all other elements for 2 hours.

(xvi) Age with 12V. on heater for 2 hours.

Fig. 8 shows a processed tube. Ionization gauges attached to several of these indicated that the pressure after processing was approximately 2×10^{-7} mm. of Hg. Typical steady state gun characteristics for this tube are shown in fig. 6.

3.3 The Periodic Magnet Structures

Two periodic magnet structures were assembled. The first consisted of six series opposing electromagnets with soft iron pole pieces, while the second consisted of a series of eleven opposing permanent magnedure (3) magnets with soft iron pole pieces. Outline drawings of these structures are given in figs.9 and 10 while photographs of the completed structures are given in figs. 11 and 12. Both structures were supported in suitable frames which also served to hold the tube central in the structure. Provision was made for adjusting the centering of the tube.

With the electromagnet structure peak magnetic fields on the axis of 0 to 450 gauss were obtainable by varying the current from 0 to 3 A. Both the magnetic field as a function of distance (see fig. 13) and peak magnetic field as a function of current were measured using a magnetic field strength meter employing the Hall effect in germanium (1). The field strength meter was calibrated against a Grassot fluxmeter. These measurements showed that the peak magnetic field was almost linear with current for the range 0 to 3 A and was given by

$$B_o \text{ (gauss)} = 150\, I_{magnet} \text{ (amp.)}$$

Fig. 13 shows the magnetic field on the axis as a function of distance for this structure which had a period of 5.72 cm. The dimensionless parameter A is given by

$$A = 9.13 \times 10^{-3} \frac{B_o^{\,2} \text{ (gauss)}}{V_{beam} \text{ (volts)}}$$

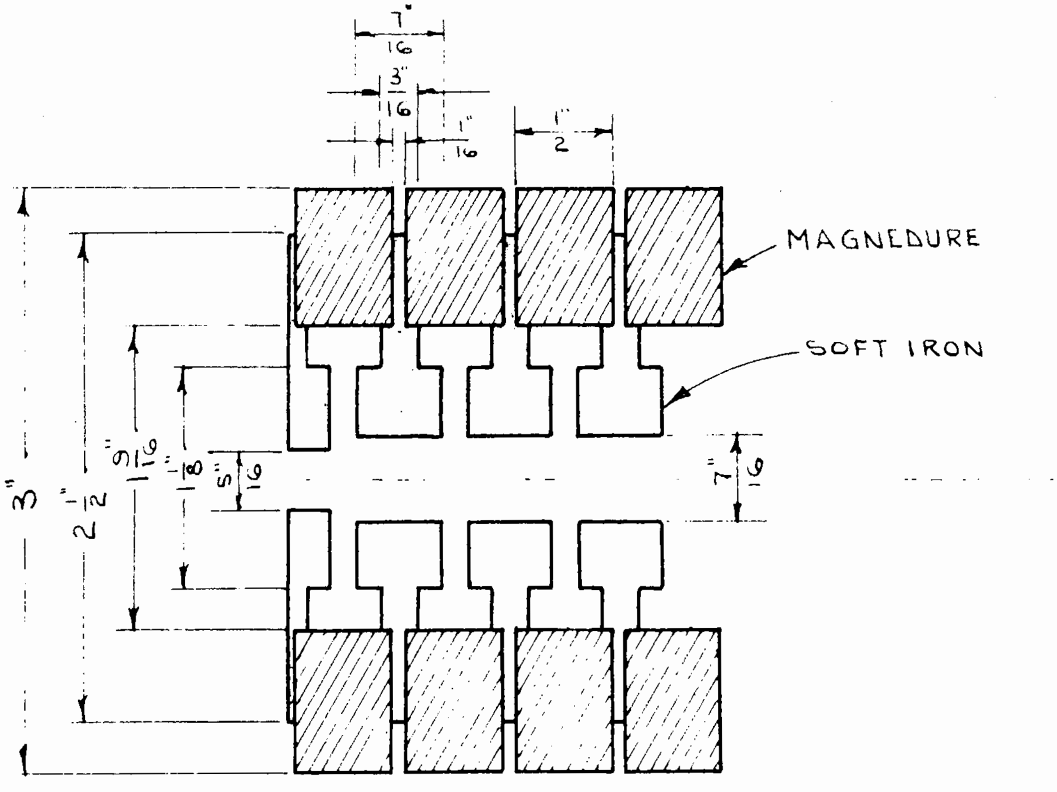

FIG. 10

THE PERMANENT MAGNET STRUCTURE

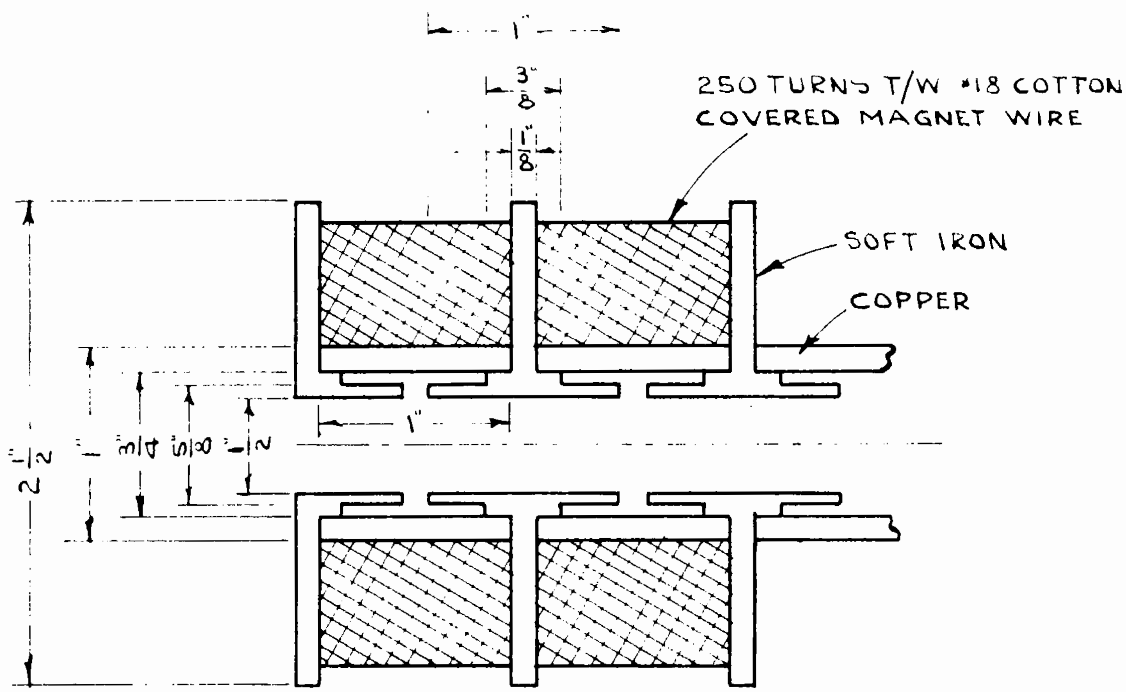

FIG. 9

THE ELECTROMAGNET STRUCTURE

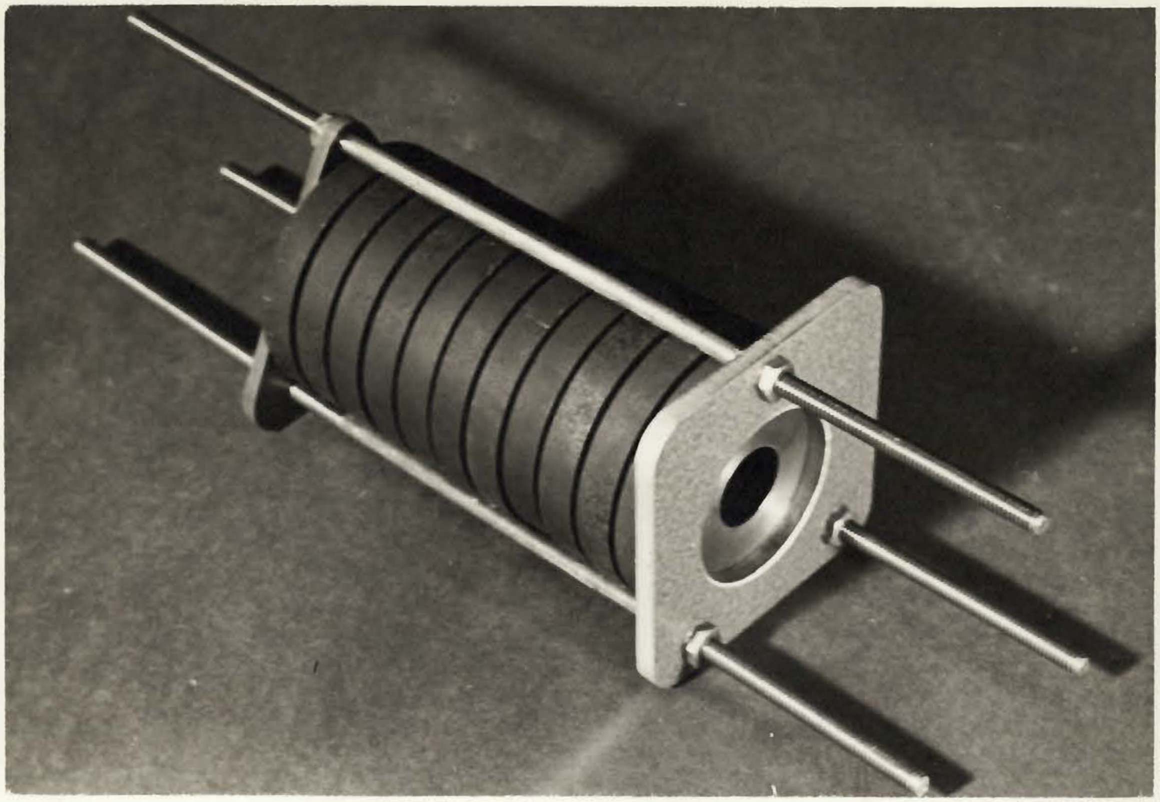

FIG. 12

THE PERMANENT MAGNET STRUCTURE

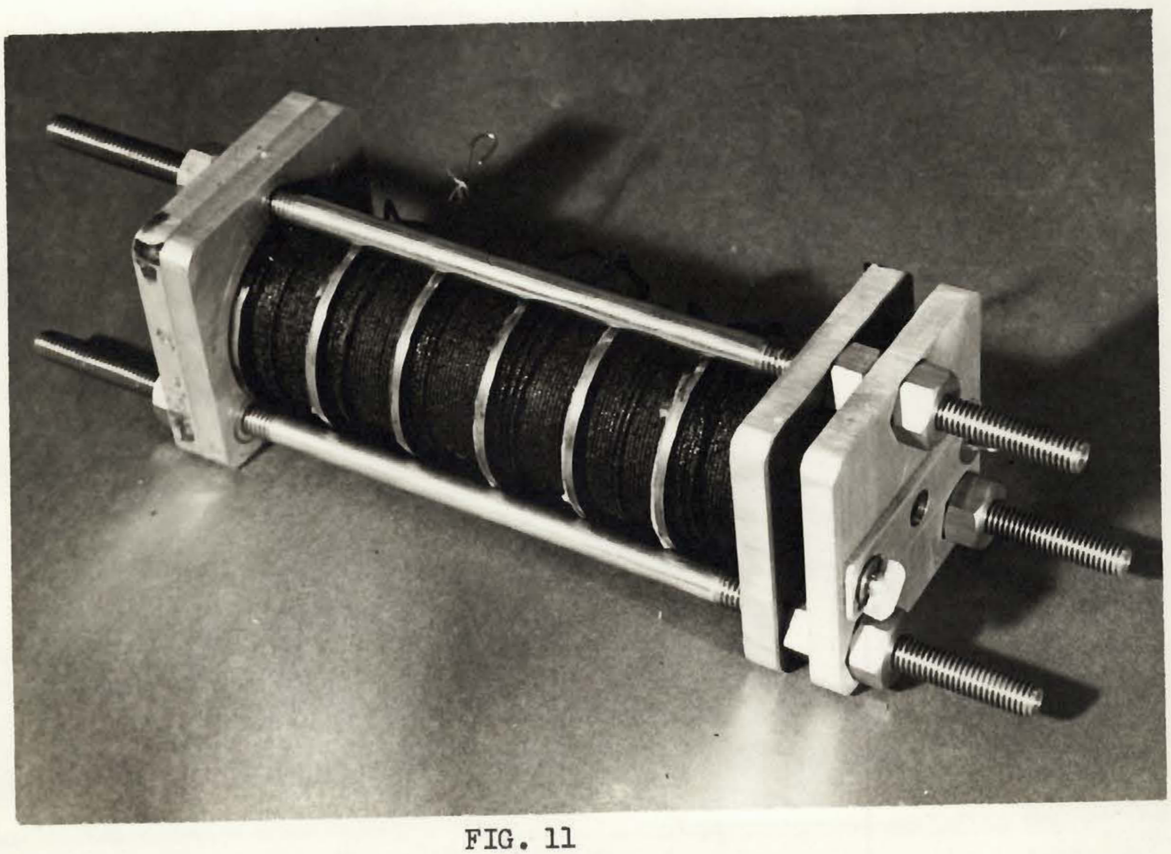

FIG. 11

THE ELECTROMAGNET STRUCTURE

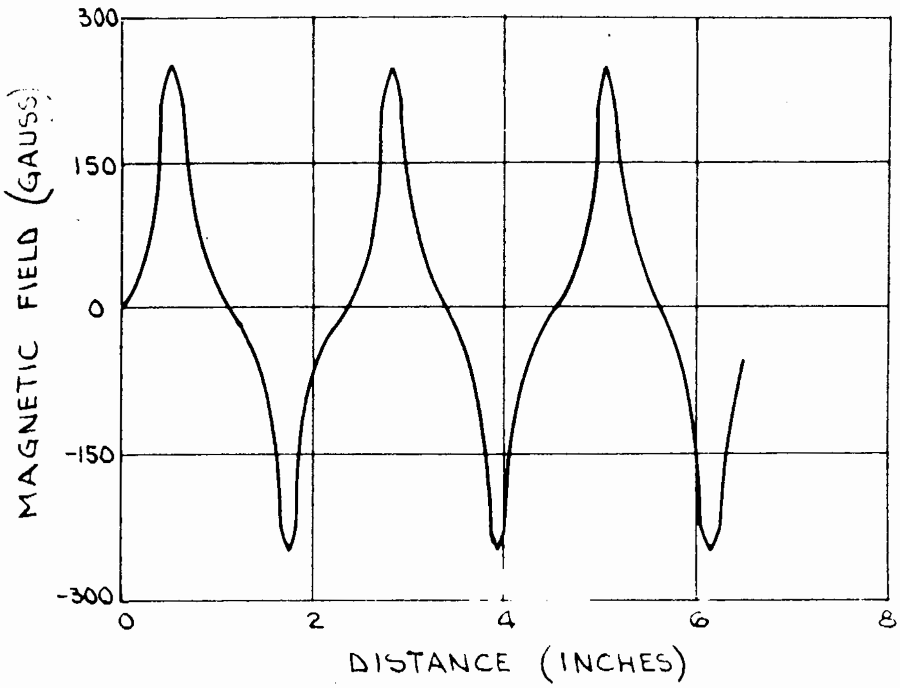

FIG 13

MAGNETIC FIELD FOR THE ELECTROMAGNET

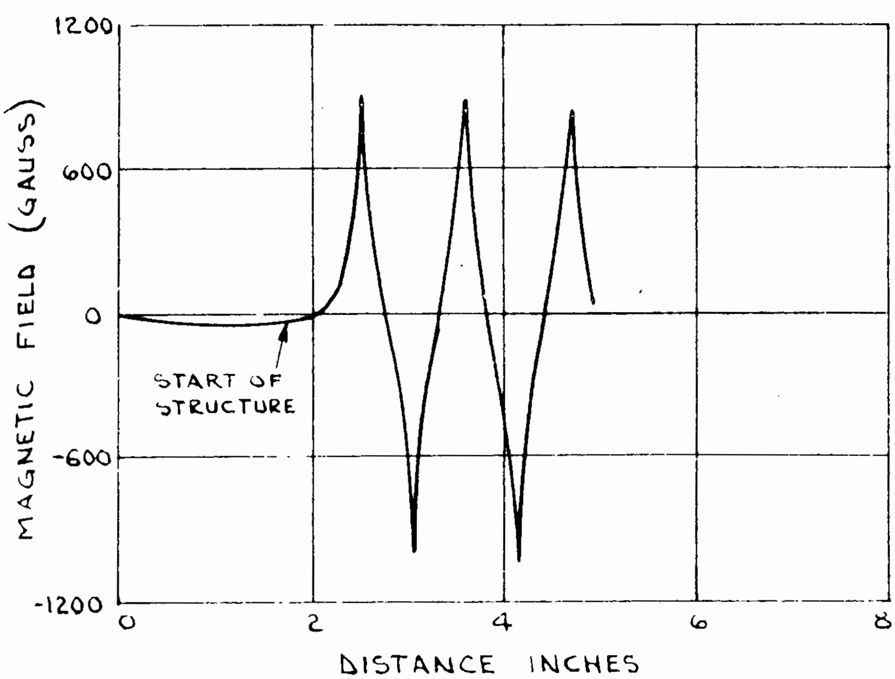

FIG 14

MAGNETIC FIELD FOR THE PERMANENT MAGNET

$$A = 2.05 \times 10^2 \frac{I^2_{magnet}\ (\text{amps})}{V_{beam}\ (\text{volts})}$$

while the dimensionless parameter B is given by

$$B = \frac{5.02 \times 10^3}{d_{beam}(\text{mm.})} \frac{I_{beam}\ (\text{milliamps})}{V^{3/2}_{beam}\ (\text{volts})}$$

The permanent magnet structure provided a fixed peak magnetic field on the axis of 980 gauss and had a period of 2.79 cm. Fig. 14 shows the magnetic field on the axis as a function of distance. The dimensionless parameter A for this structure is given by

$$A = 2.08 \times 10^3 \frac{1}{V_{beam}(\text{volts})}$$

while the dimensionless parameter B is given by

$$B = \frac{1.20 \times 10^3}{d^2_{beam}(\text{mm.})} \frac{I_{beam}\ (\text{milliamps})}{V^{3/2}_{beam}\ (\text{volts})}$$

It is interesting to note that this structure gives a constant field of 40 gauss on the axis as well as the periodic field.

3.4 The Associated Circuits

The beam voltage was obtained from a laboratory built regulated power supply which provided from 100 D.C.V. to 2500 D.C.V. output at a maximum current of 100 mA. The positive side of this supply was grounded. For the pulsed measurement this supply was coupled with a clamp type pulser built by R. McFarlane of this Laboratory. The internal multivibrator in this pulser was adjusted to give a pulse recurrence time of 1000 μsec, and the pulse length was adjustable from 0 to 100 μsec. The grid voltage was obtained from an electrically isolated battery pack which provided from 0 D.C.V. to 120 D.C.V. Meters were provided to indicate gun anode current, drift space current, and collector current. A Tektronix scope was used to display the pulsed measurements. The complete associated circuit is shown schematically in fig. 15 while a photograph of the complete experimental set-up is shown in fig. 16 a,b.

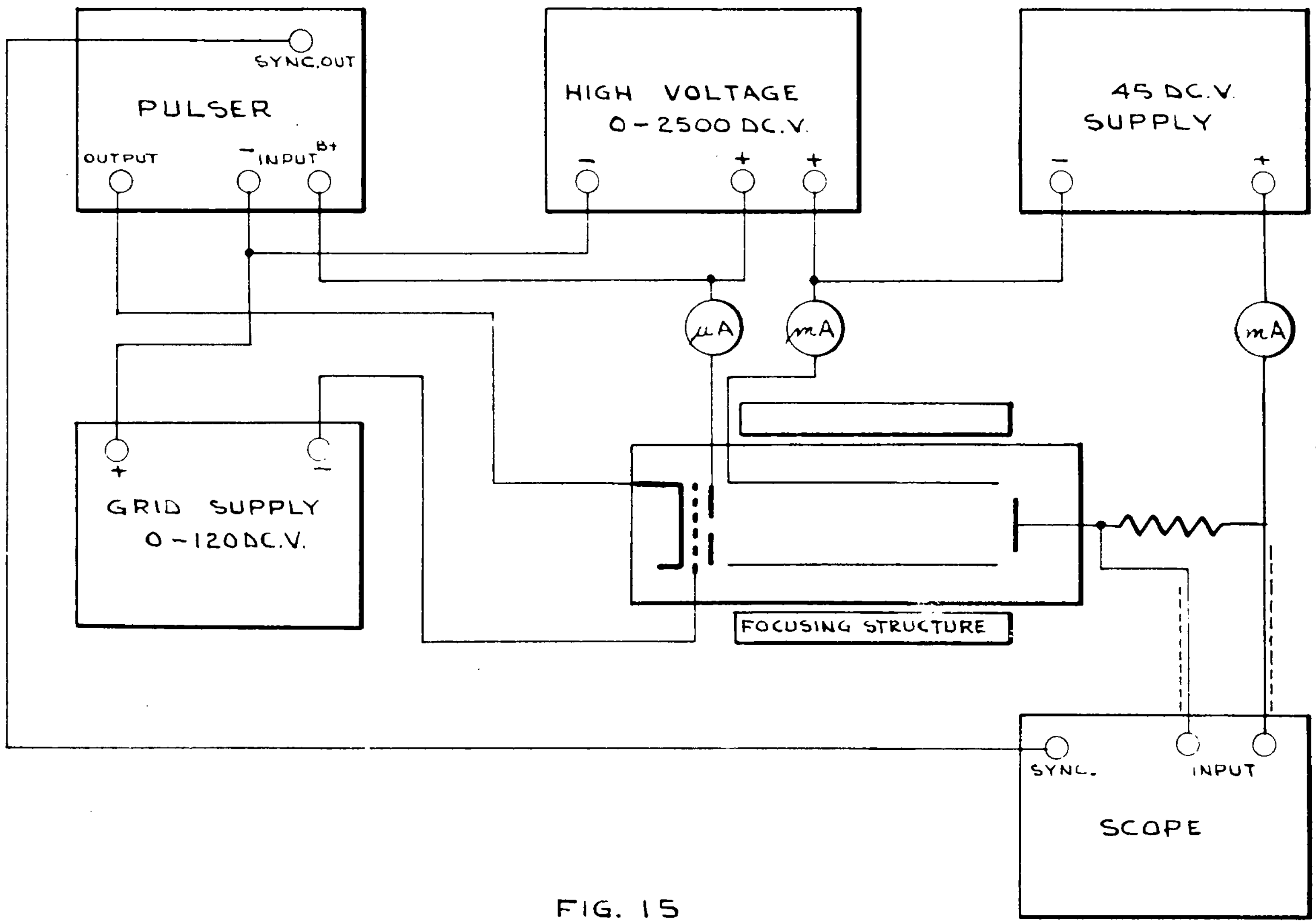

FIG. 15

BLOCK DIAGRAM OF THE ASSOCIATED CIRCUITS

FIG. 16a
THE EXPERIMENTAL APPARATUS

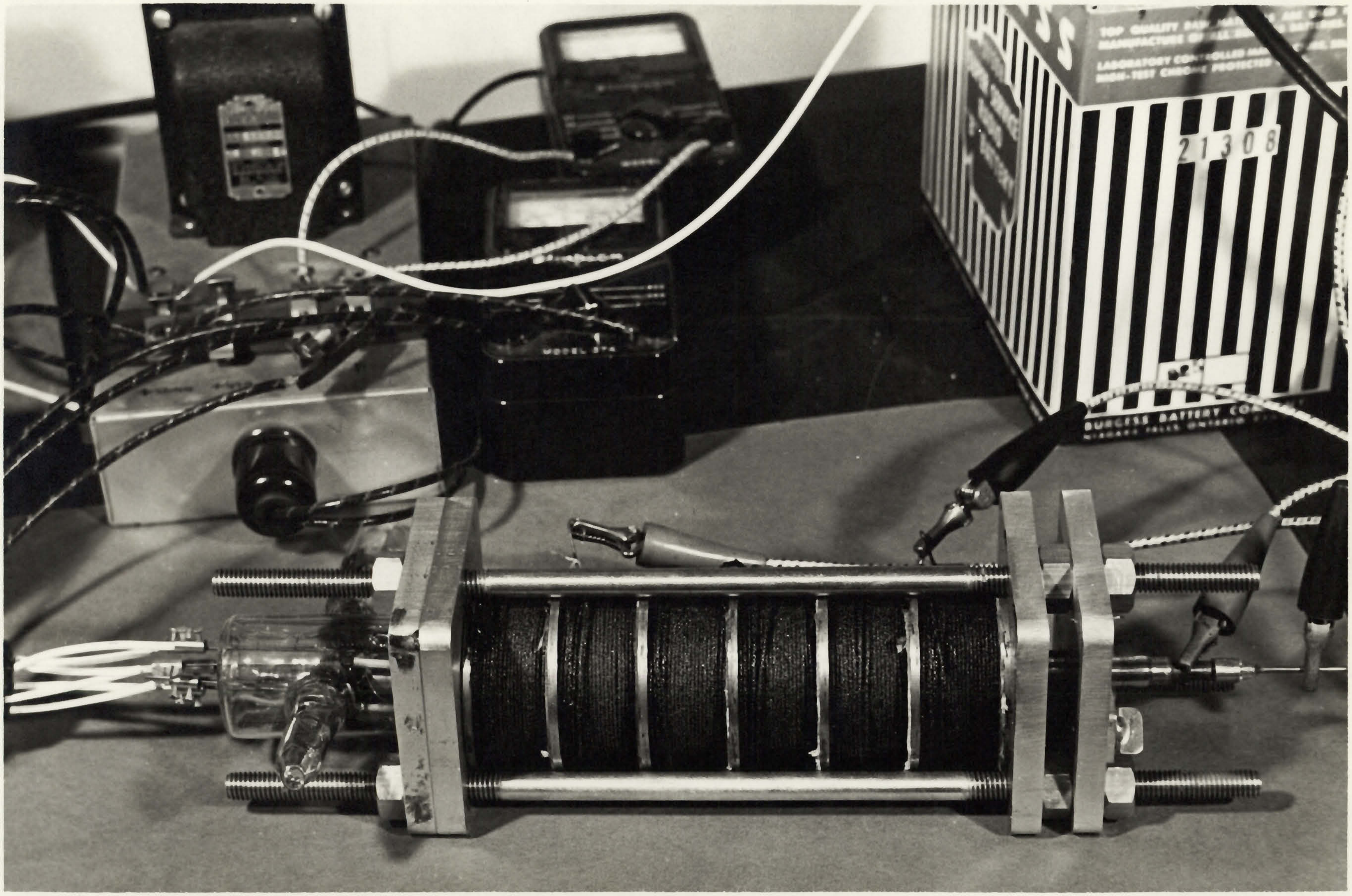

FIG. 16b

CLOSE-UP SHOWING EXPERIMENTAL TUBE IN THE ELECTROMAGNET STRUCTURE

IV. EXPERIMENTAL RESULTS

The theory, which is only valid for the magnetic field parameter A less than .6, predicts that: (1) The per cent of the beam current which arrives at the collector is a function of the magnetic field parameter A and the space charge parameter B only. Therefore, if B is held constant, the collector current is a function of A only. (2) There is a particular relation between A and B for maximum per cent of the beam current arriving at the collector. This relationship shows that larger values of B will require larger values of A. Steady state measurements were made in which B was varied in a systematic way in order to determine the dependence of the per cent of the beam current collected as a function of A (less than .6) and also to determine the manner in which the magnitude of A varies with B for a given per cent of the beam current collected. Steady state measurements were also made to determine the dependence of per cent current collected as a function of A for values of A greater than .6. Experimental studies of the initiation of the beam were made by using pulse measurements.

4.1 Steady State Measurements

4.1.1 Steady State Measurements for A Less Than .6

The space charge parameter B is proportional to the perveance of the beam $\frac{I_{beam}}{V_{beam}^{3/2}}$ and inversely proportional to the square of the beam radius. The operation of the experimental tube is such that if the gun is space charge limited and if all the electrode voltages are increased or decreased by a common factor, then both the beam perveance and the beam input radius are unchanged. Fig. 6 shows that only when the anode voltage is less than 1000 V and the grid voltage is greater than the voltage at which the knee in the anode current (I_a) versus the grid voltage (E_g) curve occurs will the gun be space charge limited. The data in table 2, which was obtained from fig. 6,

E_{drift}	E_a	E_g (knee)	E_a/E_g (knee)	$\frac{I_{beam}}{V_{beam}^{3/2}}$
Drift tube voltage	Anode voltage	Grid voltage		Beam perveance
300V	300V	15V	20	$.23 \times 10^{-6}$ $\frac{\text{amp}}{\text{volt}}$
500	500	25	20	$.27 \times 10^{-6}$
700	700	35	20	$.26 \times 10^{-6}$
900	900	45	20	$.27 \times 10^{-6}$

Table 2

illustrates this type of tube performance. Thus when the tube is used in this manner, one will be certain that B will remain constant.

In view of the fact that B is a function of beam perveance and beam input radius, a change in either of these parameters will in general produce a variation in B. In the experimental tube there are three electrode voltages (the drift tube voltage, the anode voltage and the grid voltage) which can be changed and which will produce a change in the beam perveance and/or the beam input radius. The two methods used in the experimental work are as follows: Method (1). The grid and anode voltages were changed in proportion and the drift tube voltage was changed in an arbitrary manner. This will cause the beam perveance to change but will leave the beam input radius unchanged if the change in lensing action of the drift tube is neglected (this is a second order effect). Method (2). The anode and drift tube voltage were held constant and the grid voltage changed. This causes both perveance and beam input radius to change.

The value of the magnetic field parameter A, used as the independent variable in the experimental work, is a function of the peak magnetic field and the beam voltage (i.e. the drift tube voltage). For values of A less than .8 the electromagnet structure was used and A was varied by adjusting the current supplied to the electromagnet coils. In latter experimental work described in the next sub-section where A was greater than .8, the permanent magnet structure was used. In this case A was varied by continuously changing the beam voltage.

In fig. 17 the per cent current collected is plotted against the current supplied to the coil of the electromagnet (I_{mag}) for three different values of the anode voltage. The grid and drift tube voltage were adjusted to keep B constant throughout the three curves. The data in fig. 17 is replotted in fig. 18 with the parameter A as abscissa. It is clear from this figure that the per cent current collected is a function of A only for constant B.

In fig. 19 the per cent current collected is plotted against the current supplied to the coils of the electromagnet for three different values of the drift tube voltage. The grid and anode voltage were adjusted according to method (1) described above. Since by this method beam input radius remains constant, B will be proportional to the beam perveance only. The data in fig. 19 is replotted in fig. 20 with the parameter A as abscissa. The curves clearly show that larger values of B will require larger values of A to achieve the same per cent current collected. The value of A required is, however, considerably larger than predicted by the theory. This is probably due to thermal velocity spreading in the beam which is neglected in the theory.

As a result of conclusions drawn in the preceding paragraphs, one can say that: (1) if the value of A required to achieve a given per cent current collected is the same, then B must be constant. Hence, either the beam perveance and the beam input radius squared remain constant or the beam input radius squared varies inversely as the beam perveance. At constant beam voltage this reduces to the fact that the beam input radius squared varies inversely as the beam current. (2) If the value of A required to achieve a given per cent current

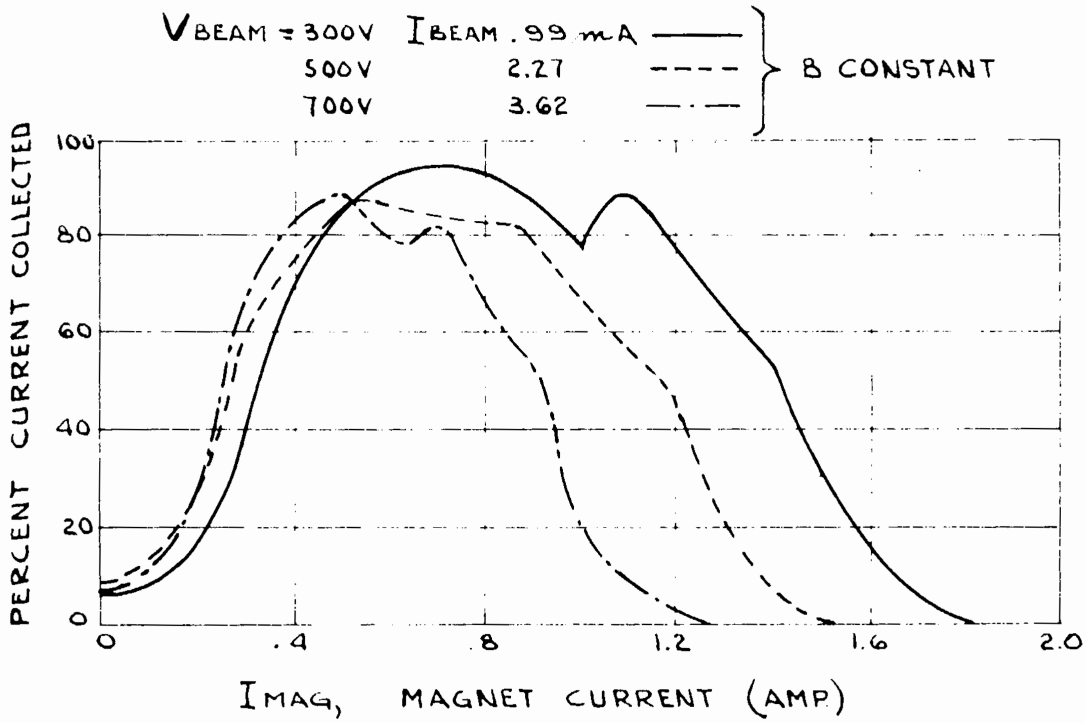
VBEAM = 300V IBEAM .99 mA
500V 2.27
700V 3.62
B CONSTANT
PERCENT CURRENT COLLECTED
100
80
60
40
20
0
0
.4
.8
1.2
1.6
2.0
IMAG, MAGNET CURRENT (AMP)

FIG. 17

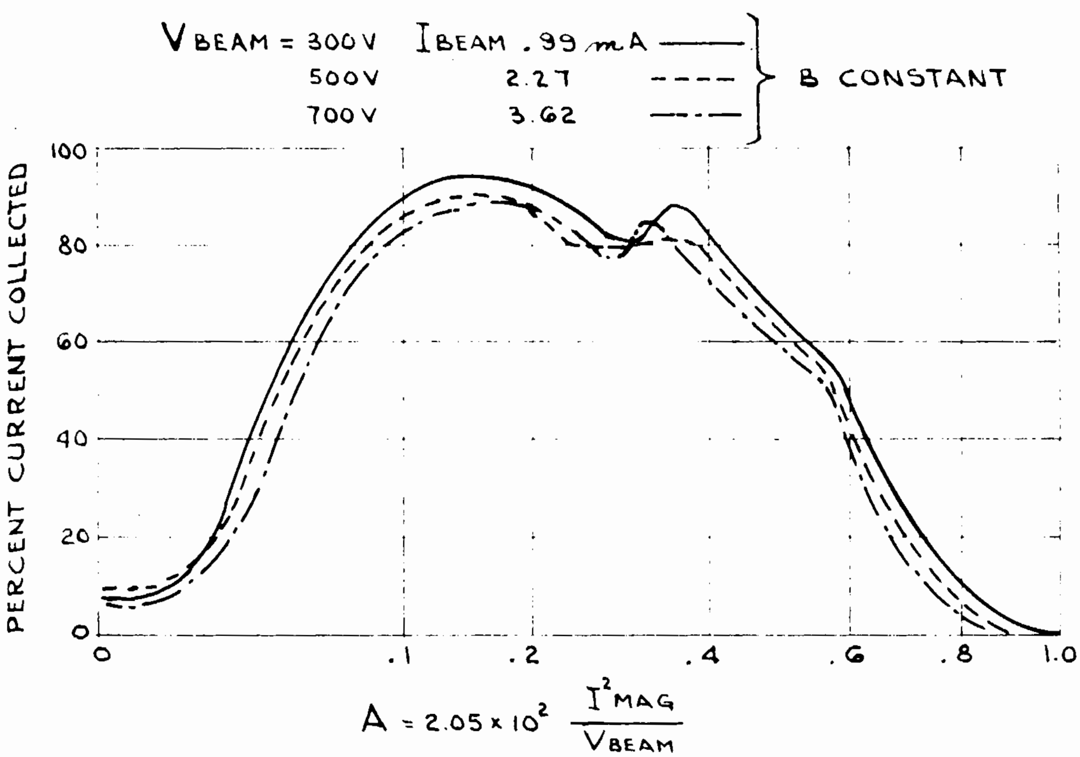
VBEAM = 300V IBEAM .99 mA
500V 2.27
700V 3.62
B CONSTANT
PERCENT CURRENT COLLECTED
100
80
60
40
20
0
0
.1
.2
.4
.6
.8
1.0
A = 2.05 x 10² I²MAG / VBEAM

FIG. 18

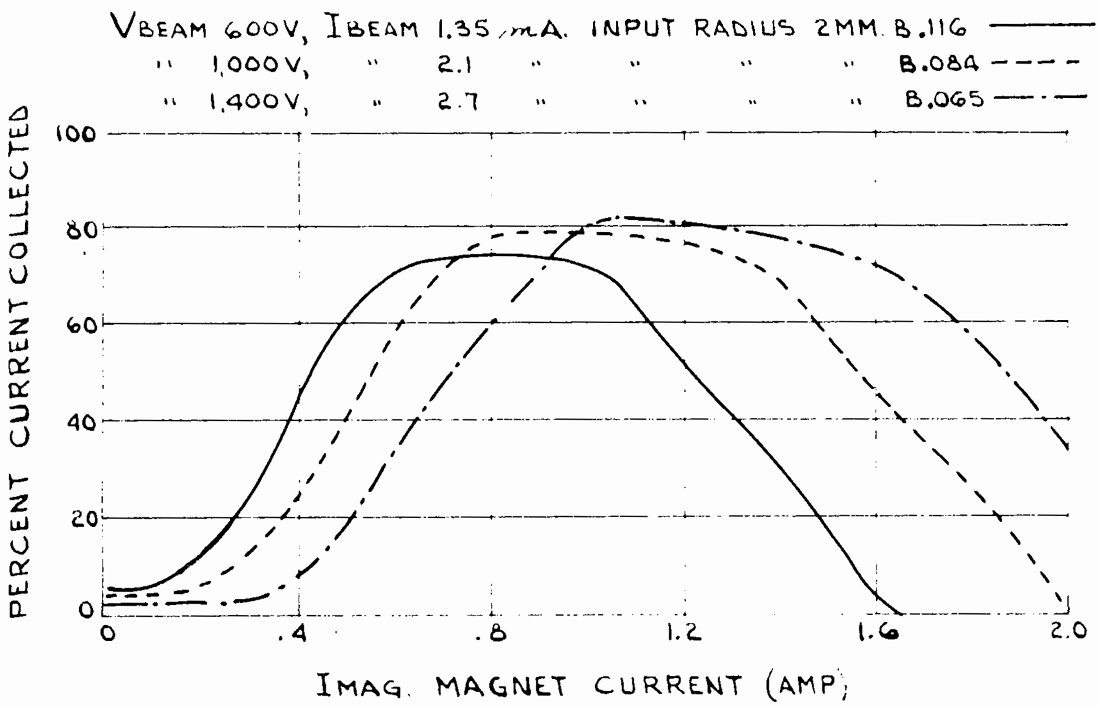

FIG 19

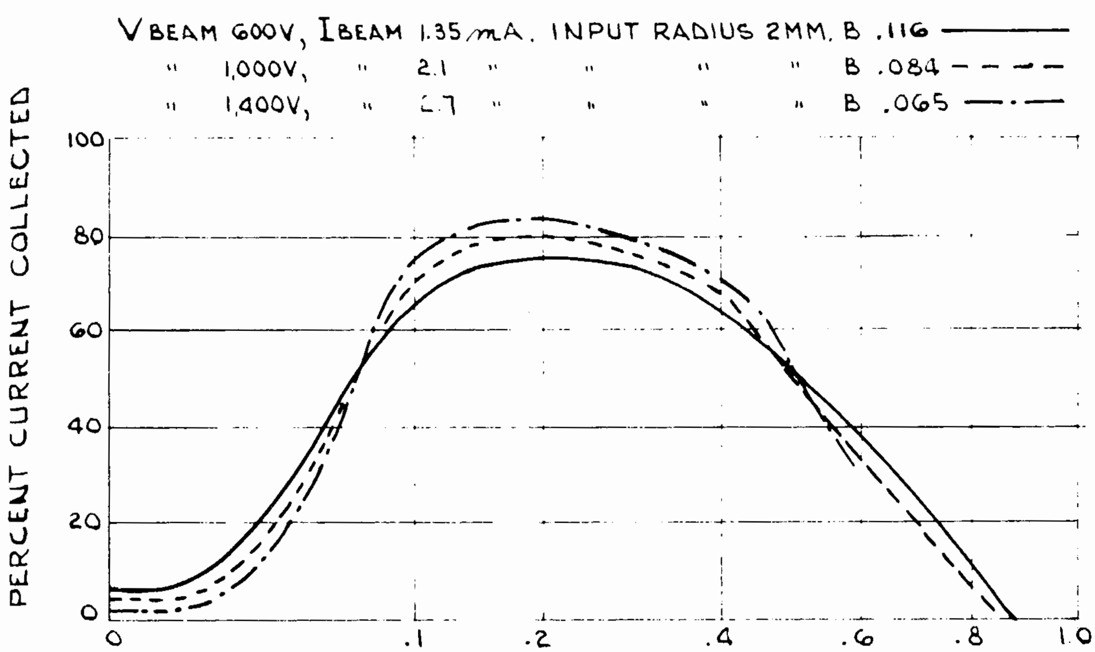

$$A = 2.05 \times 10^2 \frac{I^2_{MAG}}{V_{BEAM}}$$

FIG. 20

collected is smaller, then B must be smaller. At constant voltage this reduces to the fact that the beam input radius squared increases more rapidly than the beam current.

In fig. 21 the per cent current collected is plotted against the current supplied to the coils of the electromagnet for three different values of beam current. Method (2) described above was used to alter the beam current. The data in fig. 21 is replotted in fig. 22 with the parameter A as abscissa. Here one sees that the beam input radius squared increases more rapidly than the beam current.

4.1.2 Steady State Measurements for A Greater than .6

In order to measure the per cent current collected for values of A greater than .6, the permanent magnet structure was used. In fig. 23 the percent current collected is plotted against the beam voltage for three different gun voltage settings. The data obtained in fig. 23 is replotted in fig. 24 with the parameter A as abscissa. It is found that the per cent current collected increases and then decreases in the range A equals 0.8 to A equals 2.0. In the previous work (see for example fig. 22) it was found that the per cent current collected increased then decreased in the region A equals 0.0 to A equals 0.8. Thus one sees that the per cent current collected alternately increases and decreases as a function of A. This is known as a band pass dependence and is found for other systems with periodic symmetry.

4.1.3 Hysteresis Effects in the Electromagnet

The per cent current collected is very sensitive to small changes in the peak magnetic field. This is seen in the work described previously. As a result of this, effects were apparent which were due to hysteresis in the soft iron pole pieces. In fig. 25 the per cent current collected is plotted as a

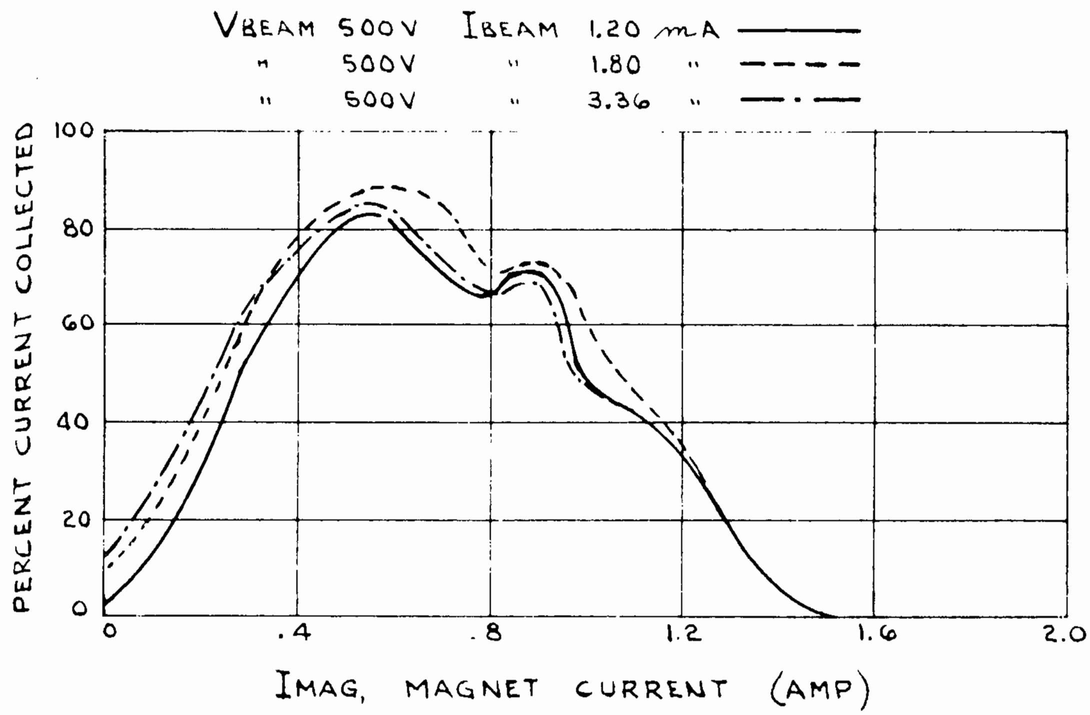
VBEAM 500V IBEAM 1.20 mA
" 500V " 1.80 "
" 500V " 3.36 "
PERCENT CURRENT COLLECTED
100
80
60
40
20
0
0
.4
.8
1.2
1.6
2.0
IMAG, MAGNET CURRENT (AMP)

FIG. 21

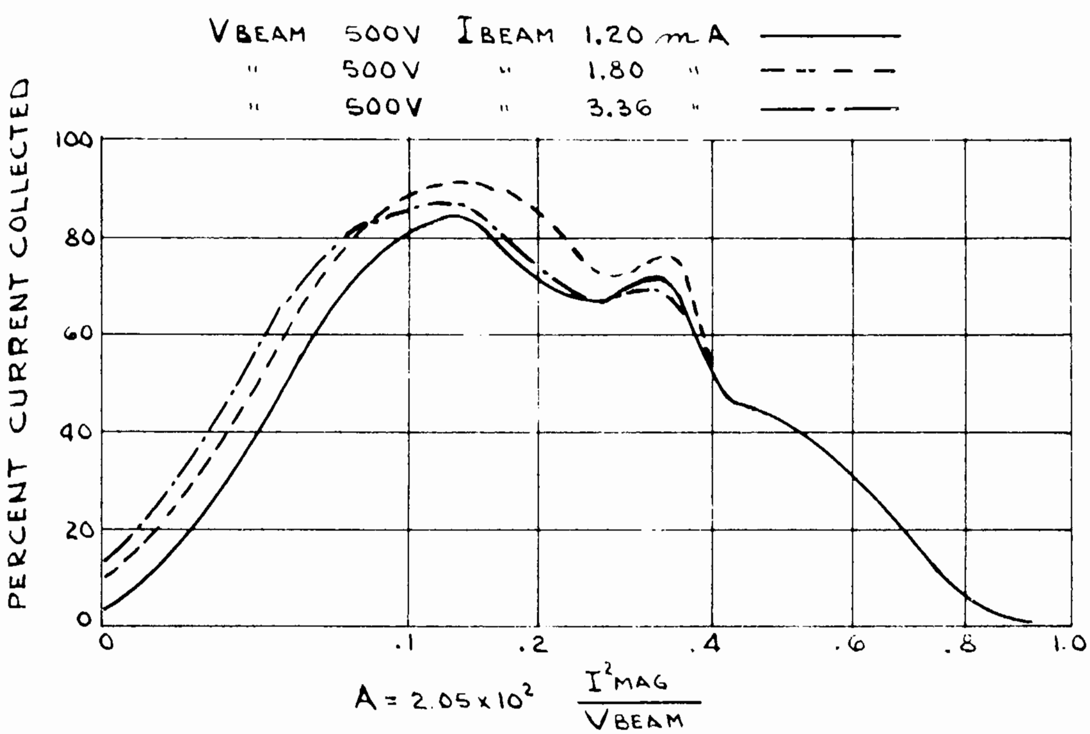
VBEAM 500V IBEAM 1.20 mA
" 500V " 1.80 "
" 500V " 3.36 "
PERCENT CURRENT COLLECTED
100
80
60
40
20
0
0
.1
.2
.4
.6
.8
1.0
$A = 2.05 \times 10^2 \frac{I^2_{MAG}}{V_{BEAM}}$

FIG. 22

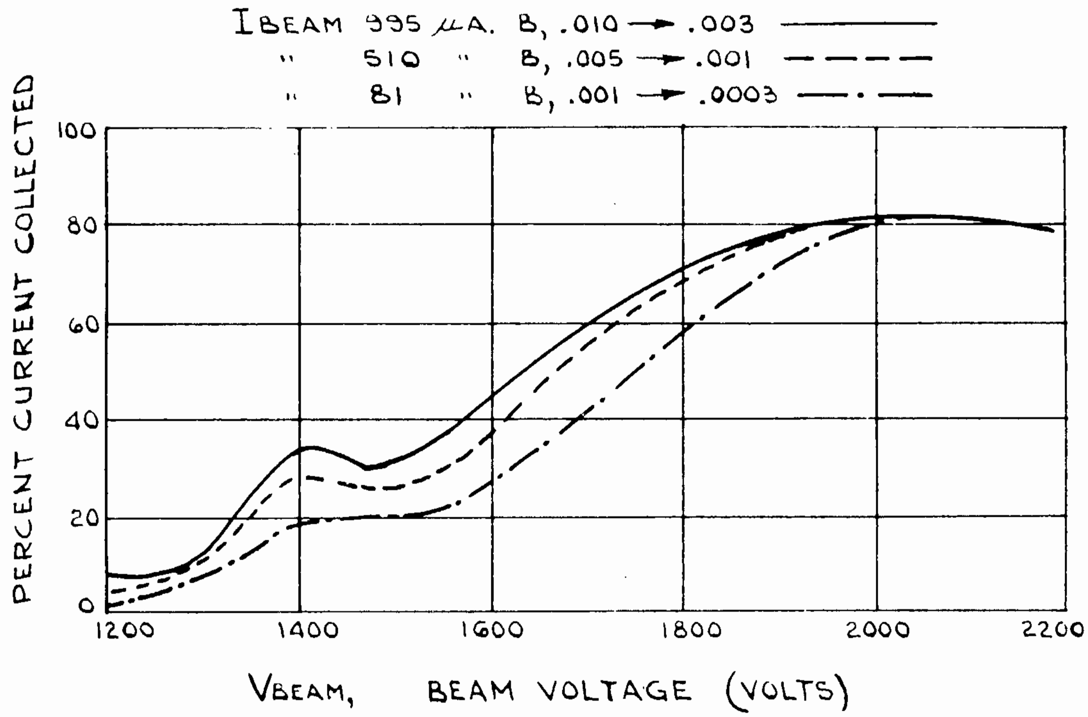
IBEAM 995 μA. B, .010 → .003
" 510 " B, .005 → .001
" 81 " B, .001 → .0003
PERCENT CURRENT COLLECTED
100
80
60
40
20
0
1200
1400
1600
1800
2000
2200
VBEAM, BEAM VOLTAGE (VOLTS)

FIG. 23

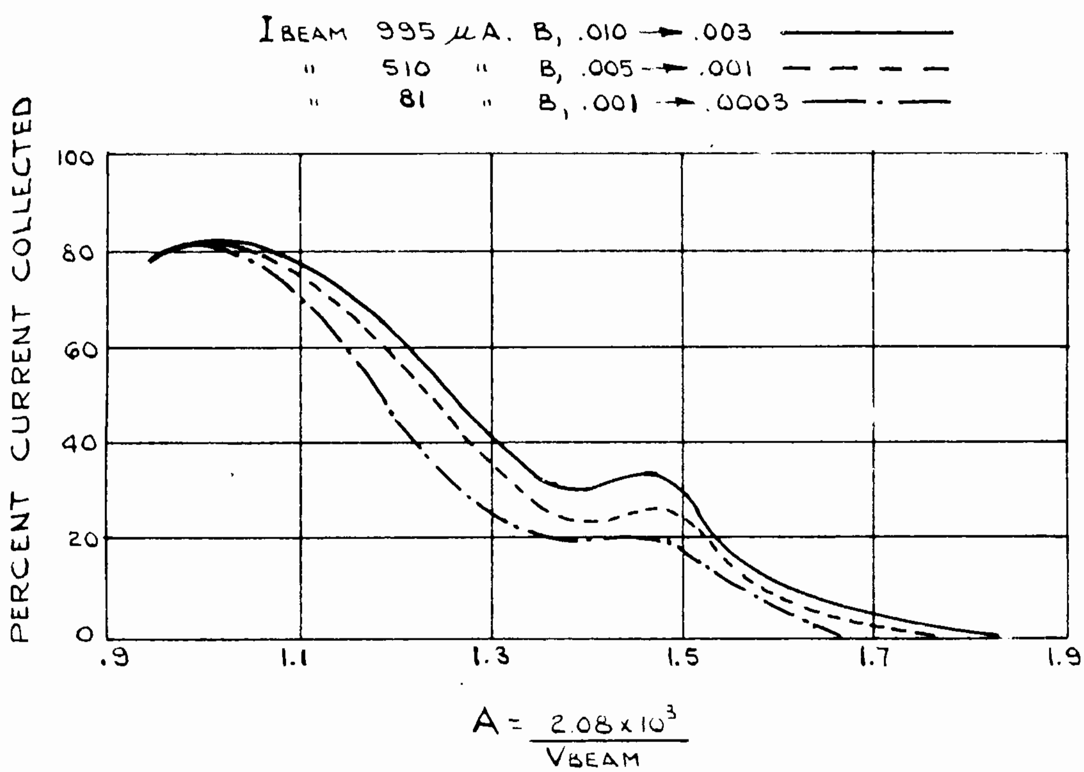
IBEAM 995 μA. B, .010 → .003
" 510 " B, .005 → .001
" 81 " B, .001 → .0003
PERCENT CURRENT COLLECTED
100
80
60
40
20
0
.9
1.1
1.3
1.5
1.7
1.9
A = 2.08 x 10³ / VBEAM

FIG. 24

function of the current supplied to the electromagnet structure (I_{mag}) for the I_{mag} increasing and decreasing directions. This data is replotted in fig. 26 with the parameter A as abscissa. It is seen that the results are not constant but depend to some extent on the past behaviour of the electromagnet structure. To remove this effect in the experimental work, all measurements were taken in the I_{mag} increasing direction. After each run the small residual magnetism was removed by applying a 60 cycle A.C. voltage to the electromagnet and slowly reducing this voltage to zero. These difficulties could be removed by using an A.C. supply for the electromagnet and a synchronously driven recorder to measure the collected current.

4.2 Pulsed Measurements

The gun was pulsed with a 0.1 μsec rise time. Collector current as a function of time was displayed on a Tektronix scope. Several of these displays are shown in fig. 27. The collector current is typified by an exponential rise with a time constant of several microseconds followed by an equilibrium value. The transit time of the electrons down the drift tube and the transit time of the electrons around the beam are of the order of one hundredth of a microsecond. Hence, one would not attribute the delay in the rise of the collector current to electron effects. However, heavier particles which are much slower moving might account for this delay. Positive ions have transit times of the order of this effect and probably cause it. They have been neglected in the work up to this point because the measurements were essentially equilibrium measurements.

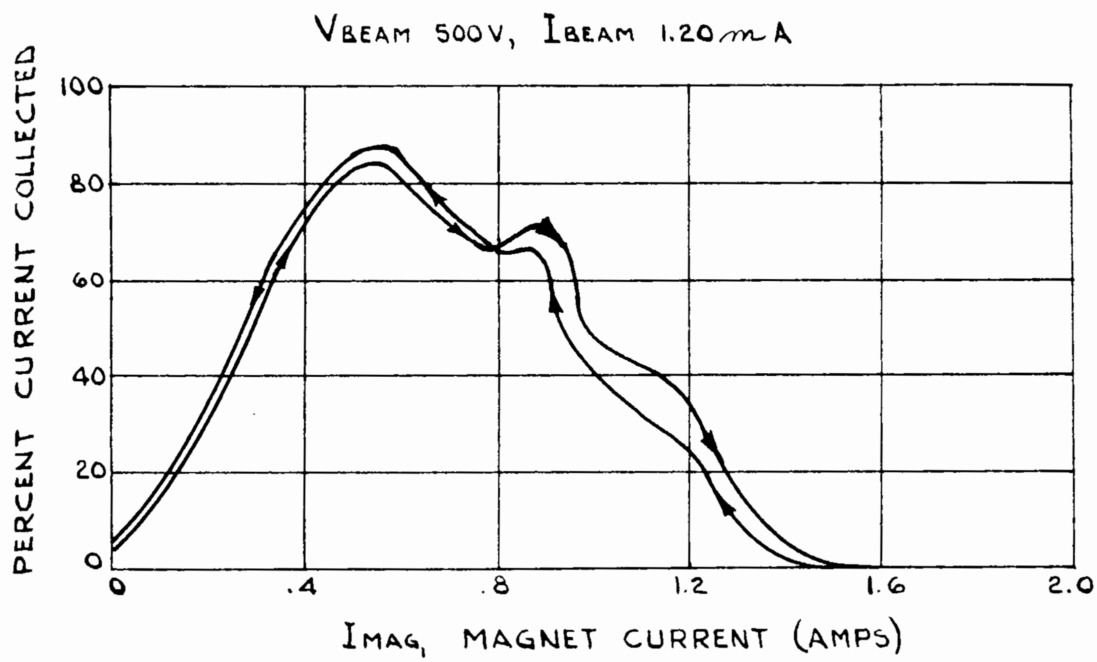
VBEAM 500V, IBEAM 1.20 mA
PERCENT CURRENT COLLECTED
100
80
60
40
20
0
0
.4
.8
1.2
1.6
2.0
IMAG, MAGNET CURRENT (AMPS)

FIG. 25

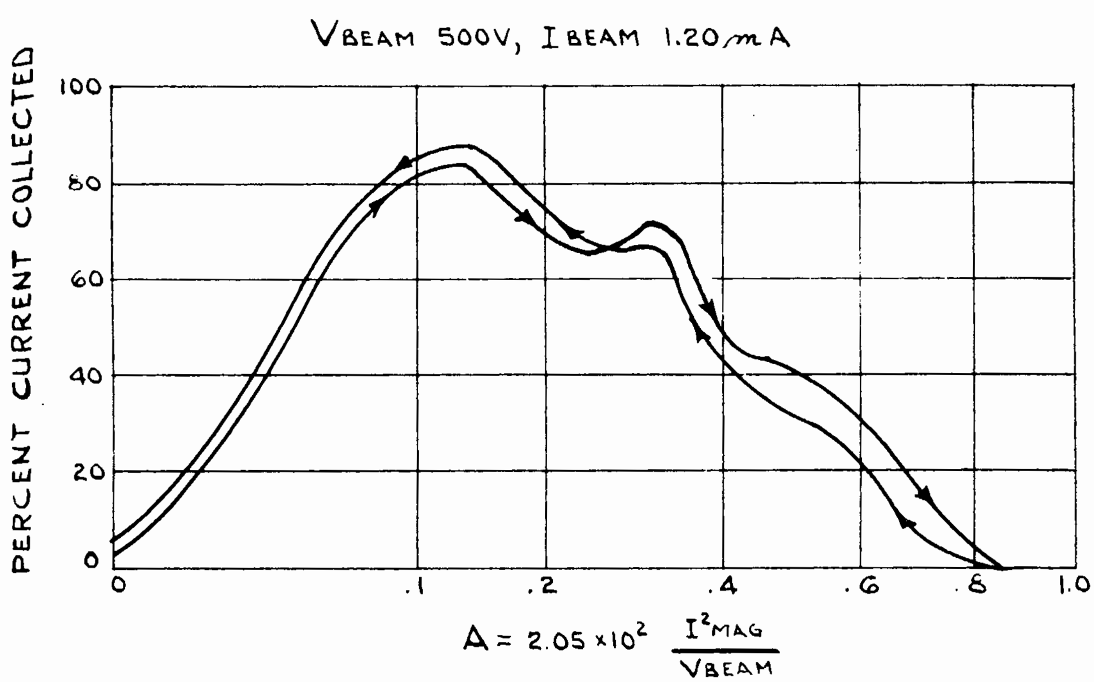
VBEAM 500V, I BEAM 1.20 mA
PERCENT CURRENT COLLECTED
100
80
60
40
20
0
0
.1
.2
.4
.6
.8
1.0
A = 2.05 × 10² I²MAG / VBEAM

FIG. 26

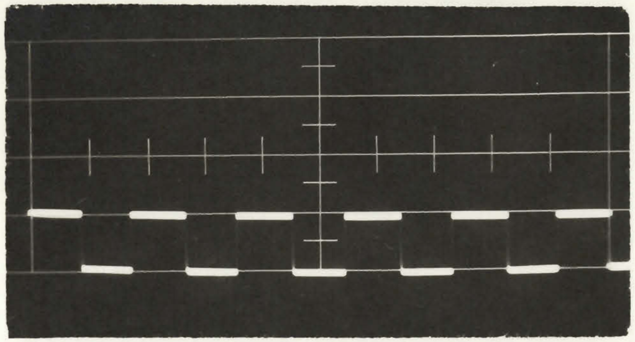

CALIBRATION 1.5mA

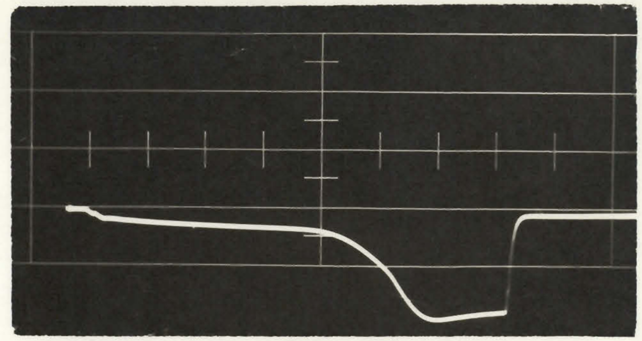

E_B 500 E_G 40 Imag .6

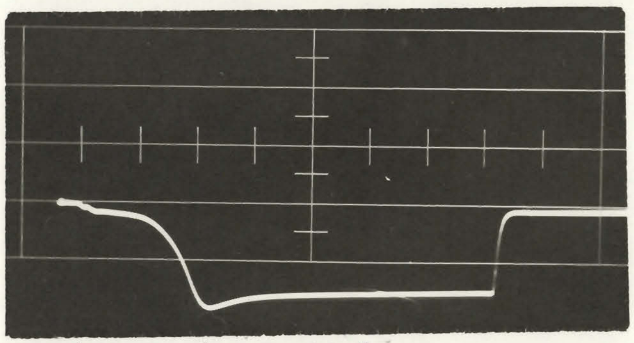

E_B 500 E_G 60 Imag .6

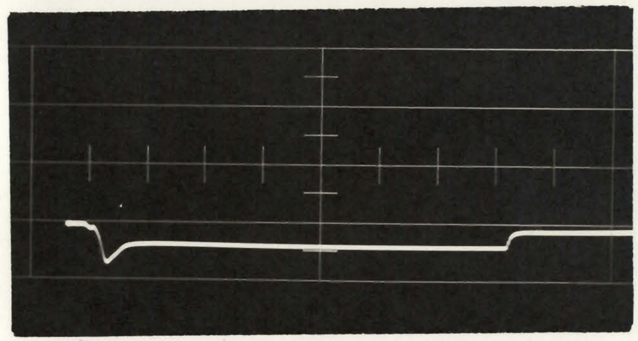

E_B 400 E_G 80 Imag .6

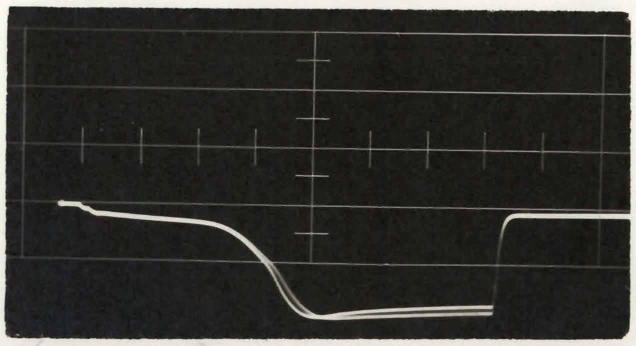

E_B 500 E_G 50 Imag .6

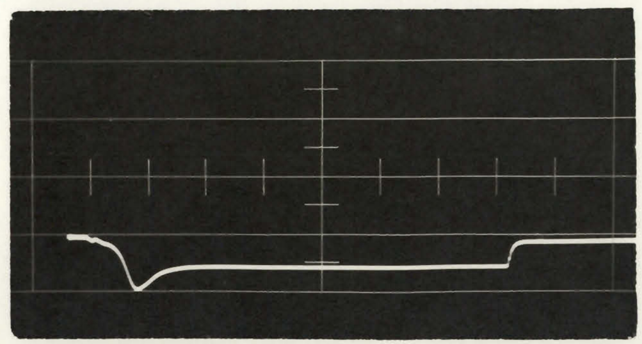

E_B 400 E_G 70 Imag .6

FIG. 27
TEKTRONIX SCOPE DISPLAYS OF PULSED MEASUREMENTS

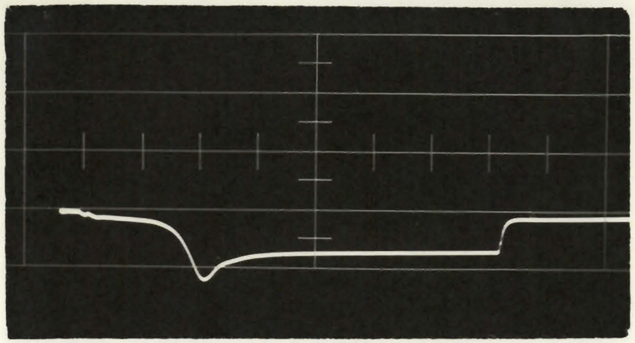

E_B 400 E_G 60 Imag .6

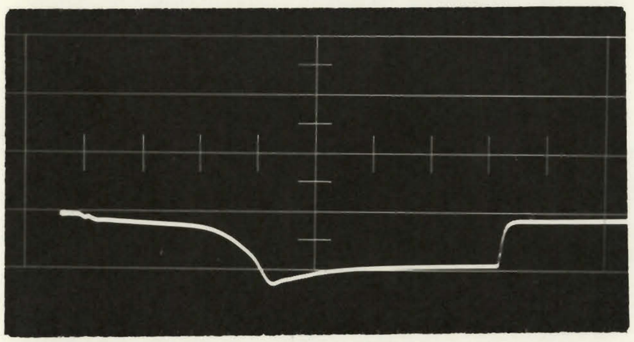

E_B 400 E_G 50 Imag .6

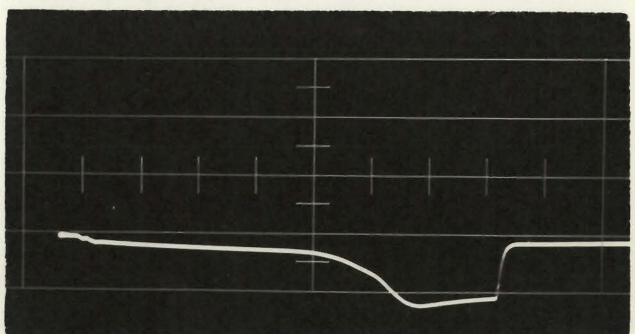

E_B 400 E_G 40 Imag .6

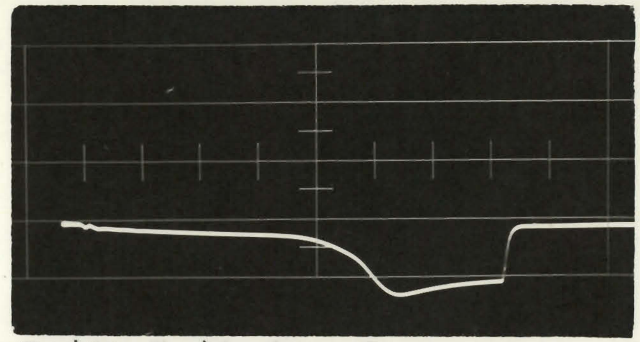

E_B 400 E_G 40 Imag .3

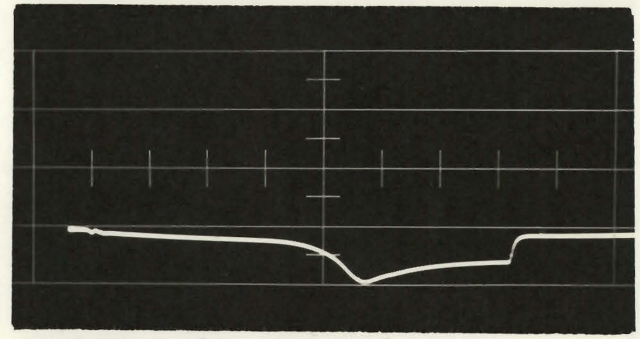

E_B 300 E_G 40 Imag .3

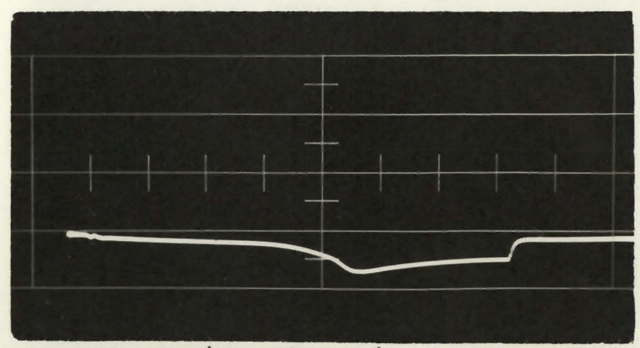

E_B 300 E_G 40 Imag .6

FIG. 27 (CONT.)
TEKTRONIX SCOPE DISPLAYS OF PULSED MEASUREMENTS

V. SUMMARY AND CONCLUSIONS

The theory as presented in section II predicts that if the focusing field and beam are characterized by two parameters A and B proportional to the magnetic field squared over the beam voltage and the beam current over the beam voltage to the three halves power respectively, then good focusing will take place when A is approximately equal to B. The theory also predicts that beams characterized by the same parameter B will focus the same under the influence of the periodic magnetic field. Both these conditions have been checked experimentally. It was found that considerably higher values of A were needed than predicted by theory. This is due to the fact that the theory ignores thermal velocity spreading. The second condition above was found to be satisfied.

It was pointed out that the assumption of laminar flow caused the theory to be invalid for values of A larger than .5. A band structure, that is, alternate regions of good transmission and no transmission, were found experimentally. This is typical of systems with periodic symmetry and is also found for periodically loaded transmission lines and wave guides.

The theory ignores the presence of positive ions. Experimentally it was found, however, that positive ions play an important part in the initiation of the beam. Much could be learned from efforts to extend the theory to include the effects of positive ions and experiments designed to measure their effects.

Periodic magnetic field focusing is practical for maintaining cylindrical electron beams of moderate perveance. Considerable weight saving can be achieved over the use of uniform magnetic field focusing by this method.

VI. ACKNOWLEDGEMENTS

The author wishes to thank the Chairman of the Department of Physics, Dr. G.A. Woonton, and his Research Director, Dr. S. Wagner, for their aid and encouragement during the course of the work described. Many valuable discussions about the work were had with Mr. R.A. McFarlane and Dr. C.R. Crowell. The help of Mr. R. Lorimer in the glass blowing and of Mr. V. Avarlaid and his workshop staff in construction of the equipment are also much appreciated.

The computer was made available by the United States Air Force under Contract No. AF 19(122)-81 to the Eaton Electronics Research Laboratory. The author wishes to express his gratitude to Mr. G.W. Farnell who assisted in the computer work.

This project formed part of the work on the physics of electron beams and of high frequency tubes which is financed by the Defence Research Board at the Eaton Electronics Research Laboratory of McGill University under the Consolidated Grant DRB 9512-20.

VII. BIBLIOGRAPHY

Periodicals

1. Pearson
A Magnetic Field Strength Meter Employing the Hall Effect in Germanium
Rev. of Sc. Inst. Apr. 48

2. Wang, C.C.
Electron Beams in Symmetrical Fields
Proc. I.R.E. 38, p. 135 Feb. 50

3. Went, J.T., Rathenau, G.W., Gorter, E.W., and Van Oosterhaut, G.W.
Ferroxdure, A Class of New Permanent Magnet Materials
Philips Tech. Rev. 13 Jan. 52

4. Courant, E.D., Livingston, M.S., and Snyder, H.S.
The Strong Focusing Synchroton
Phys. Rev. 88, p. 1190 Dec. 52

5. Pierce, J.R.
Spatially Alternating Magnetic Fields for Focusing Low-Voltage Electron Beams
J.A.P. 24, p. 1247 (L) Sept. 53

6. Brewer, G.R.
On the Focusing of High Current Electron Beams
J.A.P. 25, p. 243 Feb. 54

7. Mendel, J.T., Quate, C.F., and Yocom, W.H.
Electron Beam Focusing with Periodic Permanent Magnet Fields
Proc. I.R.E. 42, p. 800 May 54

8. Clogston, A.M. and Heffner, H.
Focusing of an Electron Beam by Periodic Fields
J.A.P. 25, p. 436 Apr. 54

9. Chang, K.K.N.
Beam Focusing by Periodic and Complementary Fields
Proc. I.R.E. 43, p. 62 Jan. 55

10. Mendel, J.T.
Magnetic Focusing of Electron Beams
Proc. I.R.E. 43, p. 327(L) Mar. 55

11. Chang, K.K.N.
Optimum Design of Periodic Magnet Structures for Electron Beam Focusing
R.C.A. Rev. XVI, p. 65 Mar. 55

12. Szabo, A.
Investigations of Magnetically Focused Electron Beams
McGill University M.Sc Thesis Aug. 55

13. Chang, K.K.N.
Periodic Magnetic Field Focusing for Low Noise Traveling Wave Tubes
R.C.A. Rev. XVI, p. 423 Sept. 55

14. Siekanowicz, W.W., and Sterzer, F.
A Developmental Wide Band, 100 Wat,, 20 Db., S Band Traveling Wave Amplifier Utilizing Periodic Permanent Magnets
Proc. I.R.E. 44, p. 55 Jan. 56

Books

15. Zworykin, V.K., Morton, G.A., Ramberg, E.G., Hillier, J., and Vance
Electron Optics and the Electron Microscope
John Wiley Co. Ltd. 1945

16. Spangenberg, K.R.
Vacuum Tubes
McGraw-Hill Book Co. 1948

17. Pierce, J.R.
Theory and Design of Electron Beams
Van Nostrand Co. Second Ed.1954